



# Absorbing boundary conditions for nonlinear acoustics: The Westervelt equation.

Igor Shevchenko<sup>a,\*</sup>, Barbara Kaltenbacher<sup>b</sup>

<sup>a</sup>*Department of Mathematics, Imperial College London, London, SW7 2AZ, UK*

<sup>b</sup>*Institute of Mathematics, Alpen-Adria-Universität Klagenfurt, Klagenfurt, A-9020, Austria*

---

## Abstract

We consider the Westervelt equation in an unbounded domain and propose nonlinear absorbing boundary conditions for its efficient and robust numerical simulations. We use the theory of pseudo- and para-differential operators as well as asymptotic expansions to derive local in space and time absorbing boundary conditions of low to high orders in a consistent way. We show that the pseudo- and para-differential theories lead to essentially the same absorbing boundary conditions in terms of computational efficiency and numerical accuracy, whereas the asymptotic expansions result in exactly the same boundary conditions as the ones obtained with the para-differential approach. Moreover, we demonstrate that the use of pseudo- and para-differential operators leads to the same boundary conditions if the nonlinear function to be linearized vanishes at zero. The numerical studies demonstrate both the efficiency and effectiveness of the developed boundary conditions for different regimes of wave propagation in a wide range of excitation frequencies and angles of incidence.

*Keywords:* Absorbing boundary conditions, Westervelt equation, Nonlinear acoustics, Pseudo-differential operators, Para-differential operators

---

## 1. Introduction

Many problems in science and engineering are naturally formulated in unbounded domains; typical examples originate from fluid dynamics, solid mechanics, aerodynamics, electrodynamics, acoustics, etc. However, numerical simulations of such problems require a finite computational region. There are basically two approaches which can be used to reformulate problems in infinite domains as problems in finite domains. The first one is to map an unbounded domain to a bounded one, known as the Perfectly Matched Layer technique first introduced by Berenger [11] and later on used for many different partial differential equations. We specifically refer to e.g., [31, 1, 34, 14, 2, 4, 16, 5, 41, 9] in the context of acoustic wave equations. The second approach, followed in this work, is to impose fictitious boundaries to truncate the domain of interest. Such artificial boundaries require special boundary conditions so that the boundary value problem is well-posed and its solution is an accurate approximation to the restriction of the solution in the unbounded domain. In other words, these boundary conditions have to be transparent to or, as they are usually called, absorbing for solutions propagating outwards the artificial boundary.

It is commonly recognized that absorbing boundary conditions (ABCs) play a key role in computations on unbounded domains and have a significant impact on the accuracy of numerical methods. Over the past thirty years,

---

\*Corresponding author

Email address: [i.shevchenko@imperial.ac.uk](mailto:i.shevchenko@imperial.ac.uk) (Igor Shevchenko)

15 ABCs have developed into a vigorous research direction including a wide spectrum of methods and approaches. A  
16 detailed description of these techniques is out of the scope of this work and therefore we restrict ourselves to referring  
17 the reader to the comprehensive review articles [23, 53, 26, 27, 24, 25] and the references therein.

18 Despite the intensive research activity in the field of transparent boundary conditions, most results have been  
19 obtained for linear problems with constant coefficients. Wave equations with variable coefficients have received  
20 much less attention, not to mention nonlinear models. There are only few papers devoted to problems with variable  
21 coefficients [20], convective [10] and nonlinear [30, 51, 59, 46] terms. Despite the existence of some approaches to  
22 the construction of ABCs for nonlinear wave models their application to concrete equations is rather sophisticated and  
23 still out of the scope of most research works.

24 The focus of this work is on the construction of ABCs for high-intensity ultrasound waves governed by the Westervelt  
25 equation, which is a basic mathematical model of nonlinear acoustics playing a central role in many medical and  
26 industrial applications, such as diagnostic ultrasound [21, 50, 47], thermotherapy of tumors [22, 28, 15], lithotripsy [6],  
27 ultrasound cleaning and sonochemistry (e.g. [17, 39]), etc. Linear acoustic models are not applicable to high intensity  
28 ultrasound regimes of wave propagation due to appearing nonlinear effects, which require more sophisticated wave  
29 equations to be taken into account.

30 The ABCs proposed in this work are based on two approaches: the theory of pseudo-differential [40, 32, 45] and  
31 para-differential [36, 44] calculus. The first approach is applicable to linear wave equations with variable coefficients,  
32 therefore we use it for the Westervelt equation linearized in a neighborhood of a reference solution. The second  
33 approach we apply directly to the nonlinear Westervelt equation. Notice that both the pseudo- and para-differential  
34 theories have already been used in the construction of transparent boundary conditions. For example, the pseudo-  
35 differential calculus was exploited by Engquist and Majda in [20] to design ABCs for the linear wave equation with  
36 variable coefficients. Another application of the pseudo-differential calculus to the construction of ABCs for the  
37 acoustic wave equation can be found in [8]. The pseudo-differential approach has also been used to derive ABCs  
38 for optical waveguides [7] and the Maxwell equations [3]. Transparent boundary conditions for the semilinear wave  
39 equation as well as for the nonlinear Schrödinger equation were obtained in [52] and [51], respectively, with the help  
40 of para-differential operators.

41 The novelty of our work lies in the derivation and analysis of high-order ABCs for the Westervelt equation,  
42 which have not yet been constructed. We do so for the one- and two-dimensional versions of the Westervelt equation  
43 first of all in a domain without corners. It is worth noting that ABCs in general and for the Westervelt equation in  
44 particular are used not only when computational domains are infinitely large but also when they are too large for  
45 numerical simulations. Specifically, the High Intensity Focused Ultrasound (HIFU) problem considered in this work  
46 is a striking example where a finite but still so vast domain of wave propagation occurs that using the entire domain  
47 would make computations unfeasible. In the HIFU problem, the use of ABCs is inevitable, since they allow to carry  
48 out simulations in domains of order of centimeters (where are the most interesting physical processes take place),  
49 otherwise it would require to consider a much larger computational domain to guarantee that the waves leaving the  
50 domain were attenuated enough not to influence the physical processes studied.

51 The rest of this paper is organized as follows. In Section 2 we present the problem formulation. In Section 3  
52 we derive absorbing boundary conditions for the Westervelt equation, in one and two space dimensions, based on  
53 the pseudo- and para-differential calculus as well as on asymptotic expansions. Section 4 focuses on the Lagrange  
54 multiplier based technique to couple the Westervelt equation and ABCs, and on numerical methods to solve the  
55 coupled problem. In Section 5 we give numerical results demonstrating the efficiency of the proposed boundary  
56 conditions. The paper concludes with a discussion of the main findings.

## 57 2. Problem definition

58 The Westervelt equation is one of the fundamental equations governing the propagation of acoustic waves in  
59 nonlinear regimes [55, 28, 15, 13]. This equation was first derived from Lighthill's equation by Westervelt [55]. In  
60 this work, we present a brief derivation of the Westervelt equation from the basic equations of fluid dynamics: the  
61 continuity equation, the Navier–Stokes equation, the entropy equation, and the equation of state.

62 We introduce the pressure  $p$ , density  $\rho$ , velocity  $\mathbf{v}$ , specific entropy  $s$ , and temperature  $T$ , and decompose these

63 quantities into their time-mean and fluctuating components as

$$p = p_0 + p', \quad (1)$$

$$\rho = \rho_0 + \rho', \quad (2)$$

$$\mathbf{v} = \mathbf{v}_0 + \mathbf{v}', \quad (3)$$

$$s = s_0 + s', \quad (4)$$

$$T = T_0 + T'. \quad (5)$$

64 To derive the Westervelt equation, we first consider the equation of continuity

$$\rho_t + \mathbf{v} \cdot \nabla \rho + \rho \nabla \cdot \mathbf{v} = 0. \quad (6)$$

65 Substitution of (1) and (2) into (6) gives

$$(\rho_0 + \rho')_t + \mathbf{v} \cdot \nabla(\rho_0 + \rho') + (\rho_0 + \rho') \nabla \cdot \mathbf{v} = 0. \quad (7)$$

66 Assuming the time-mean density  $\rho_0$  to be constant, one can rewrite (7) as

$$\rho'_t + \rho_0 \nabla \cdot \mathbf{v} = -\rho' \nabla \cdot \mathbf{v} - \mathbf{v} \cdot \nabla \rho'. \quad (8)$$

67 To proceed, we make use of the Navier–Stokes equation

$$\rho(\mathbf{v}_t + (\mathbf{v} \cdot \nabla)\mathbf{v}) + \nabla p = \mu \Delta \mathbf{v} + \left( \zeta + \frac{1}{3} \mu \right) \nabla(\nabla \cdot \mathbf{v}), \quad (9)$$

68 with  $\zeta$  and  $\mu$  standing for the shear and bulk viscosities, respectively.

69 Applying the vector identities

$$\nabla(\nabla \cdot \mathbf{v}) = \Delta \mathbf{v} + \nabla \times \nabla \times \mathbf{v}, \quad (10a)$$

$$\mathbf{v} \cdot \nabla \mathbf{v} = \frac{1}{2} \nabla(\mathbf{v} \cdot \mathbf{v}) - \mathbf{v} \times \nabla \times \mathbf{v}, \quad (10b)$$

71 to the Navier–Stokes equation (9) results in

$$\rho \left( \mathbf{v}_t + \frac{1}{2} \nabla(\mathbf{v} \cdot \mathbf{v}) - \mathbf{v} \times \nabla \times \mathbf{v} \right) + \nabla p = \mu \Delta \mathbf{v} + \left( \zeta + \frac{1}{3} \mu \right) (\Delta \mathbf{v} + \nabla \times \nabla \times \mathbf{v}). \quad (11)$$

72 Assuming constant  $p_0$  and using (1) and (2), we rewrite (11) in the form

$$(\rho_0 + \rho') \left( \mathbf{v}_t + \frac{1}{2} \nabla(\mathbf{v} \cdot \mathbf{v}) - \mathbf{v} \times \nabla \times \mathbf{v} \right) + \nabla p' = \mu \Delta \mathbf{v} + \left( \zeta + \frac{1}{3} \mu \right) (\Delta \mathbf{v} + \nabla \times \nabla \times \mathbf{v}), \quad (12)$$

73 which after some rearrangements leads to

$$\rho_0 \mathbf{v}_t + \frac{\rho_0}{2} \nabla(\mathbf{v} \cdot \mathbf{v}) - \rho_0 \mathbf{v} \times \nabla \times \mathbf{v} + \rho' \mathbf{v}_t + \frac{\rho'}{2} \nabla(\mathbf{v} \cdot \mathbf{v}) - \rho' \mathbf{v} \times \nabla \times \mathbf{v} + \nabla p' = \left( \zeta + \frac{4}{3} \mu \right) \Delta \mathbf{v} + \left( \zeta + \frac{1}{3} \mu \right) \nabla \times \nabla \times \mathbf{v}. \quad (13)$$

74 Applying (10b) to (13) and taking into account that the acoustic velocity  $\mathbf{v}$  is irrotational in our case ( $\nabla \times \mathbf{v} = 0$ ),  
75 equation (13) can be written in the following form

$$\rho_0 \mathbf{v}'_t + \frac{\rho_0}{2} \nabla(\mathbf{v}' \cdot \mathbf{v}') + \rho' \mathbf{v}'_t + \nabla p' = \left( \zeta + \frac{4}{3} \mu \right) \Delta \mathbf{v}', \quad (14)$$

76 where we also assume zero time-mean velocity  $\mathbf{v}_0$ , which implies the equality  $\mathbf{v} = \mathbf{v}'$ , and omit the third order  
77 fluctuating term  $\frac{\rho'_t}{2} \nabla(\mathbf{v} \cdot \mathbf{v})$ .

78 Another component needed in the derivation is the entropy equation [29]:

$$\rho T \frac{Ds}{Dt} = \kappa \Delta T + \mu (\nabla \cdot \mathbf{v})^2 + \frac{\mu}{2} \left( \frac{\partial v_i}{\partial x_j} + \frac{\partial v_j}{\partial x_i} - \frac{2}{3} \delta_{ij} \frac{\partial v_k}{\partial x_k} \right)^2, \quad (15)$$

79 where  $s$  is the specific entropy (per unit mass),  $\kappa$  is the thermal conductivity,  $T$  is the temperature, and  $\delta_{ij}$  is the  
80 Kronecker delta.

81 According to [29], the right hand side of (15) is dominated by the term  $\kappa \Delta T'$ . We therefore can write

$$\rho_0 T_0 s'_t = \kappa \Delta T'. \quad (16)$$

82 Given the equation of state in the form

$$p = p(\rho, s), \quad (17)$$

83 we expand it in a Taylor series about an equilibrium state  $(\rho_0, s_0)$  and neglect the third-order terms, namely

$$p - p_0 = (P_\rho)_{s,0} (\rho - \rho_0) + \frac{1}{2!} (P_{\rho\rho})_{s,0} (\rho - \rho_0)^2 + (P_s)_{\rho,0} (s - s_0) + \dots \quad (18)$$

84 Equation (18) can also be expressed as

$$p' = A \left( \frac{\rho'}{\rho_0} \right) + \frac{B}{2} \left( \frac{\rho'}{\rho_0} \right)^2 + (P_s)_{\rho,0} s', \quad (19)$$

85 with

$$A = \rho_0 (P_\rho)_{s,0} \equiv \rho_0 c^2, \quad B = \rho_0^2 (P_{\rho\rho})_{s,0},$$

86 where  $c$  is the speed of sound, which is assumed to be constant. Thus, equation (19) can be recast into the form

$$p' = c^2 \rho' + \frac{c^2}{\rho_0} \frac{B}{2A} \rho'^2 + (P_s)_{\rho,0} s'. \quad (20)$$

87 In order for the Westervelt equation to be independent of  $s'$ , we combine the entropy equation (16) and the  
88 continuity equation (20). In accordance with [48], we substitute  $T' = (T_p)_{s,0} p'$  into (16) that yields

$$\rho_0 T_0 s'_t = \kappa (T_p)_{s,0} \nabla \cdot \nabla p'. \quad (21)$$

89 From the linear Euler equation

$$\mathbf{v}_t = -\frac{1}{\rho_0} \nabla p', \quad (22)$$

90 we find

$$-\nabla p' = \rho_0 \mathbf{v}_t \quad (23)$$

91 and substitute it into equation (21):

$$\rho_0 T_0 s'_t = -\rho_0 \kappa (T_p)_{s,0} (\nabla \cdot \mathbf{v})_t. \quad (24)$$

92 Then, we integrate equation (24) with respect to time and have

$$\rho_0 T_0 s' = -\rho_0 \kappa (T_p)_{s,0} \nabla \cdot \mathbf{v}, \quad (25)$$

93 or

$$s' = -\frac{\kappa}{T_0} (T_p)_{s,0} \nabla \cdot \mathbf{v}. \quad (26)$$

94 Substitution of (26) into (20) yields

$$p' = c^2 \rho' + \frac{c^2}{\rho_0} \frac{B}{2A} \rho'^2 - \frac{\kappa}{T_0} (P_s)_{\rho,0} (T_p)_{s,0} \nabla \cdot \mathbf{v}. \quad (27)$$

95 In order to compute the coefficient  $\frac{1}{T_0} (P_s)_{\rho,0} (T_p)_{s,0}$  in (27), we use the equation of state for a perfect gas [48],  
 96 which gives

$$p' = c^2 \rho' + \frac{c^2}{\rho_0} \frac{B}{2A} \rho'^2 - \kappa \left( \frac{1}{c_v} - \frac{1}{c_p} \right) \nabla \cdot \mathbf{v}. \quad (28)$$

97 Using the linear equation of continuity

$$\nabla \cdot \mathbf{v} \approx -\frac{1}{\rho_0} \rho'_t. \quad (29)$$

98 in (28) results in

$$p' = c^2 \rho' + \frac{c^2}{\rho_0} \frac{B}{2A} \rho'^2 + \frac{\kappa}{\rho_0} \left( \frac{1}{c_v} - \frac{1}{c_p} \right) \rho'_t. \quad (30)$$

99 On the other hand, from the linear equation of state

$$\rho' = p' c^{-2}, \quad (31)$$

100 it follows that (30) can be written as

$$p' = c^2 \rho' + \frac{1}{\rho_0 c^2} \frac{B}{2A} p'^2 + \frac{\kappa}{\rho_0 c^2} \left( \frac{1}{c_v} - \frac{1}{c_p} \right) p'_t. \quad (32)$$

101 Multiplication of equation (32) by  $c^{-2}$  and expressing it in terms of  $\rho'$  gives

$$\rho' = \frac{p'}{c^2} - \frac{1}{\rho_0 c^4} \frac{B}{2A} p'^2 - \frac{\kappa}{\rho_0 c^4} \left( \frac{1}{c_v} - \frac{1}{c_p} \right) p'_t. \quad (33)$$

102 The next step is to combine the equation of continuity (8), the momentum equation (14) and the equation of state  
 103 (33) into one equation. For doing so, we first use (29) and (31) to recast (8) in the form

$$\rho'_t + \rho_0 \nabla \cdot \mathbf{v} = \frac{p'}{\rho_0 c^4} p'_t - \frac{1}{c^2} \mathbf{v} \cdot \nabla p'. \quad (34)$$

104 We then differentiate equation (33) with respect to time

$$\rho'_t = \frac{1}{c^2} p'_t - \frac{1}{\rho_0 c^4} \frac{B}{2A} (p'^2)_t - \frac{\kappa}{\rho_0 c^4} \left( \frac{1}{c_v} - \frac{1}{c_p} \right) p'_{tt} \quad (35)$$

105 and use (34) to have

$$\frac{1}{c^2} p'_t - \frac{1}{\rho_0 c^4} \frac{B}{2A} (p'^2)_t - \frac{\kappa}{\rho_0 c^4} \left( \frac{1}{c_v} - \frac{1}{c_p} \right) p'_{tt} + \rho_0 \nabla \cdot \mathbf{v} = \frac{1}{2\rho_0 c^4} (p'^2)_t - \frac{1}{c^2} \mathbf{v} \cdot \nabla p'. \quad (36)$$

106 Using equations (22), (31) to express the term  $\rho' \mathbf{v}'_t$  and equations (29), (31) to express the term  $(\zeta + \frac{4}{3}\mu) \Delta \mathbf{v}'$ , one  
 107 can reformulate the Navier–Stokes equation (14) as

$$\rho_0 \mathbf{v}_t + \nabla p' = \frac{1}{2\rho_0 c^2} \nabla p'^2 - \frac{\rho_0}{2} \nabla(\mathbf{v} \cdot \mathbf{v}) - \frac{1}{\rho_0 c^2} \left( \zeta + \frac{4}{3}\mu \right) \nabla p'_t. \quad (37)$$

108 Application of the divergence operator to (37) gives

$$\rho_0 (\nabla \cdot \mathbf{v}_t) + \Delta p' = \frac{1}{2\rho_0 c^2} \Delta p'^2 - \frac{\rho_0}{2} \Delta(\mathbf{v} \cdot \mathbf{v}) - \frac{1}{\rho_0 c^2} \left( \zeta + \frac{4}{3}\mu \right) \Delta p'_t. \quad (38)$$

109 Differentiation of (36) with respect to time and subtraction the resulting equation from (38) leads to

$$\begin{aligned} \Delta p' - \frac{1}{c^2} p'_{tt} &= \frac{1}{2\rho_0 c^2} \Delta p'^2 - \frac{\rho_0}{2} \Delta(\mathbf{v} \cdot \mathbf{v}) - \frac{1}{\rho_0 c^2} \left( \zeta + \frac{4}{3}\mu \right) \Delta p'_t \\ &\quad - \frac{1}{\rho_0 c^4} \frac{B}{2A} (p'^2)_{tt} - \frac{\kappa}{\rho_0 c^4} \left( \frac{1}{c_v} - \frac{1}{c_p} \right) p'_{ttt} - \frac{1}{2\rho_0 c^4} (p'^2)_{tt} - \frac{\rho_0}{2c^2} (\mathbf{v} \cdot \mathbf{v})_{tt}. \end{aligned} \quad (39)$$

110 After rearrangement of the right hand side in (39) and using the replacements

$$\Delta(\mathbf{v} \cdot \mathbf{v}) = c^{-2}(\mathbf{v} \cdot \mathbf{v})_{tt}, \quad \Delta p' = c^{-2}p'_{tt},$$

111 in the higher order terms we arrive at Kuznetsov's equation, which governs the propagation of nonlinear waves in a  
112 thermoviscous medium,

$$\frac{1}{c^2}p'_{tt} - \Delta p' - \frac{\delta}{c^4}p'_{ttt} = \left( \frac{1}{\rho_0 c^4} \frac{B}{2A} p'^2 + \frac{\rho_0}{c^2} \mathbf{v} \cdot \mathbf{v} \right)_{tt}, \quad (40)$$

113 where the diffusivity of sound  $\delta > 0$  is given, as presented in [42], by

$$\delta = \frac{1}{\rho_0} \left( \zeta + \frac{4}{3}\mu \right) + \frac{\kappa}{\rho_0} \left( \frac{1}{c_v} - \frac{1}{c_p} \right),$$

114 Assuming that local nonlinear effects can be neglected, (i.e., making the replacement  $\mathbf{v} \cdot \mathbf{v} = \left( \frac{1}{\rho_0 c} p' \right)^2$  on the right  
115 hand side) we arrive at the Westervelt equation

$$\frac{1}{c^2}p'_{tt} - \Delta p' - \frac{\delta}{c^4}p'_{ttt} = \frac{\beta_a}{\rho_0 c^2} (p'^2)_{tt}, \quad (41)$$

116 and inserting the linear wave equation relation for the damping term (i.e.  $c^{-2}p'_{ttt} = \Delta p'_t$ ), the Westervelt equation (41)  
117 can be written as

$$\frac{1}{c^2}u_{tt} - \Delta u - \frac{\delta}{c^2}\Delta u_t = \frac{\beta_a}{\rho_0 c^2} (u^2)_{tt}, \quad \text{in } (0, T) \times \Omega, \quad u := p', \quad (42)$$

118 and  $\Omega \subseteq \mathbb{R}^d$ ,  $d \in \{1, 2, 3\}$ ,  $u = u(\cdot, t)$  is the acoustic pressure,  $\beta_a = 1 + B/(2A)$  with  $B/(2A) > 0$  standing for the  
119 parameter of nonlinearity of the fluid, and  $T$  is the final time at which the problem is to be solved. All the parameters  
120 are assumed to be constant.

121 The Westervelt equation (41) is widely used to simulate high-intensity focused ultrasound fields generated by  
122 medical ultrasound transducers. This equation is valid when the cumulative nonlinear effects dominate the local  
123 nonlinear effects. Unlike the Khokhlov-Zabolotskaya-Kuznetsov equation, which is valid for directional sound beams  
124 and can be applied for transducers with relatively small aperture angles, the Westervelt equation allows using large-  
125 aperture-angle transducers.

126 In some cases the dimensionless form of the Westervelt equation [54] is more preferable than its dimensional  
127 analogue. However, for the purpose of this paper, we use the dimensional version of the equation. It is also worth  
128 noting that the classical Westervelt equation derived in [55] is an equation which is obtained from (41) by setting  
129  $\delta = 0$ . Despite this fact, equation (41) is also referred to as the Westervelt equation.

130 We recast the Westervelt equation (42) in a form more convenient for further treatment

$$c^{-2}u_{tt} - \Delta u - \beta \Delta u_t = \gamma (u^2)_{tt} \quad \text{in } (0, T) \times \Omega \quad (43)$$

131 with  $\beta = \delta/c^2$ ,  $\gamma = \beta_a/(\rho_0 c^4)$ , and complement (43) with the initial conditions

$$u(\cdot, t = 0) = u_0, \quad u_t(\cdot, t = 0) = u_1 \quad \text{in } \Omega, \quad (44)$$

132 and with the inhomogeneous Neumann and absorbing boundary conditions

$$u_n \Big|_{(0,T) \times \Gamma_N} = g(t), \quad \mathcal{A}u \Big|_{(0,T) \times \Gamma_A} = 0, \quad (45)$$

133 where  $\Gamma_N$  is a boundary part on which excitation of sound takes place, and  $\Gamma_A$  is an artificial boundary part on which  
134 absorbing boundary conditions are prescribed;  $\partial\Omega = \Gamma_N \cup \Gamma_A$ ,  $n$  is the normal derivative to the boundary  $\Gamma_N$  and the  
135 operator  $\mathcal{A}$  is an annihilating operator for outgoing waves, which we specify in due course.

### 136 3. Absorbing boundary conditions for the Westervelt equation

137 In our derivation, without loss of generality we consider two domains  $\Omega = (-\infty, 0]$  in 1-d and  $\Omega = (-\infty, 0] \times \mathbb{R}$  in  
138 2-d, where  $x$  plays the role of the outward unit normal and (in 2-d)  $y$  is the tangential direction.

139 *3.1. Absorbing boundary conditions in 1-d via linearization and pseudo-differential calculus*

140 As it was already mentioned, the direct reformulation of the Westervelt equation (43) in terms of pseudo-differential  
141 operators is not possible because of the nonlinear term on the right hand side. Therefore, we linearized (43) around a  
142 reference solution  $u^{(0)}$

$$(c^{-2} - 2\gamma u^{(0)})u_{tt} - \Delta u - \beta \Delta u_t = 2\gamma u_t^{(0)} u_t \quad \text{in } (0, T) \times \Omega. \quad (46)$$

143 After the derivation of the ABCs from this inhomogeneous linear wave equation with variable coefficients, we re-  
144 insert  $u^{(0)} = u$  to arrive at the ABCs for the Westervelt equation. The reason for using (46) (as was also done for the  
145 well-posedness proof in [37]) and not the standard linearization according to the first order Taylor expansion, which  
146 would be

$$c^{-2}u_{tt} - \Delta u - \beta \Delta u_t = 2\gamma(2u_t^{(0)}u_t + uu_{tt}^{(0)} + u^{(0)}u_{tt} - (u_t^{(0)})^2 - u^{(0)}u_{tt}^{(0)}) \quad \text{in } (0, T) \times \Omega, \quad (47)$$

147 is that the offset terms  $-2(u_t^{(0)})^2 - 2u^{(0)}u_{tt}^{(0)} = -\gamma(u^{(0)})_{tt}^2$  would destroy the commutativity of symbols of pseudo-  
148 differential operators below.

149 For simplicity of exposition we first of all consider the one-dimensional version of the Westervelt equation (43)

$$c^{-2}u_{tt} - u_{xx} - \beta u_{txx} = \gamma(u^2)_{tt}. \quad (48)$$

150 Thus, in 1-d the operator form of linearization (46) reads as

$$\mathfrak{D}_1 u = 0, \quad \text{with } \mathfrak{D}_1 = \nu^2 \partial_t^2 - \partial_x^2 - \beta \partial_{txx} - 2\gamma u_t^{(0)} \partial_t, \quad (49)$$

151 where we set  $\nu^2 = \nu^2(u^{(0)})$  with

$$\nu^2(\nu) = c^{-2} - 2\gamma \nu, \quad (50)$$

152 and point out that our analysis of the Westervelt equation, cf. [38], is based on estimates that actually make sure  
153 positivity of  $c^{-2} - 2\gamma u$ , so that  $\nu^2 > 0$  is a natural assumption. In order to derive transparent boundary conditions for  
154 the linearized Westervelt equation (48) we make use of the theory of pseudo-differential calculus. For the purpose of  
155 this formal derivation,  $\nu$  is assumed to be a  $C^\infty$  function both in time and space. Otherwise further discussion based  
156 on pseudo-differential operators makes no sense due to the impossibility to associate a differential operator with a  
157 symbol having a limited regularity. Since we do not prove this smoothness, our derivations are only formal.

158 Our derivation of ABCs is based on the Nirenberg factorization of (49) written in terms of pseudo-differential  
159 operators. Thus, to construct approximate boundary conditions we factorize the operator  $\mathfrak{D}_1$  as

$$\mathfrak{D}_1 = -(\partial_x - A)(\partial_x - B) + R, \quad (51)$$

160 where  $A = A(x, t, D_t)$  and  $B = B(x, t, D_t)$  are pseudo-differential operators with symbols  $a(x, t, \tau)$  and  $b(x, t, \tau)$  from  
161 the space

$$S^1 = S^1(\mathbb{R}^2) = \left\{ f(t, \tau) \in C^\infty(\mathbb{R}^2) : \left| \frac{\partial^\xi}{\partial t^\xi} \frac{\partial^\sigma}{\partial \tau^\sigma} f(t, \tau) \right| \leq C_{\xi, \sigma} (1 + |\tau|)^{1-|\sigma|}, \quad \forall \xi, \sigma \in \mathbb{N}_0 \right\}.$$

162 The differential operator  $D_t$  is defined as  $-i\partial_t$  with the imaginary unit  $i$ , and  $R$  is a smoothing pseudo-differential  
163 operator with the Schwartz kernel  $k(x, y) \in C^\infty$  satisfying [33]:

$$(1 + |x - y|)^N \left| \frac{\partial^\xi}{\partial x^\xi} \frac{\partial^\sigma}{\partial y^\sigma} k(x, y) \right| \leq C_{\xi, \sigma, N}, \quad \forall \xi, \sigma, N \in \mathbb{N}_0.$$

164 Developing factorization (51), we get

$$\mathfrak{D}_1 = -\partial_x^2 + (A + B)\partial_x + B_x - AB + R. \quad (52)$$

165 At the symbolic level, factorization (52) reduces to

$$\nu^2(i\tau)^2 - \beta(i\tau)\partial_x^2 - 2\gamma u_t^{(0)}(i\tau) = (a + b)\partial_x + b_x - ab + R \quad (53)$$

166 with the correspondence  $i\tau \leftrightarrow \partial_t$  between the frequency and the (physical) time domains. By a slight abuse of notation,  
 167 for a function  $f$ , we denote the symbol of the zero order differential operators  $u \mapsto fu$  (multiplication operator) again  
 168 by  $f$ .

169 The next step is to define symbols  $a$  and  $b$  in (53). For doing so, it is worth to remark that formally these symbols  
 170 admit the following asymptotic expansions

$$a(x, t, \tau) \sim \sum_{j \geq 0} a_{1-j}(x, t, \tau), \quad |\tau| \rightarrow \infty, \quad (54a)$$

171 and

$$b(x, t, \tau) \sim \sum_{j \geq 0} b_{1-j}(x, t, \tau), \quad |\tau| \rightarrow \infty, \quad (54b)$$

172 where  $a_{1-j}(x, t, \tau)$  and  $b_{1-j}(x, t, \tau)$  are homogeneous functions of degree  $1 - j$  in  $\tau$ . To asymptotically expand the  
 173 symbol  $c := ab$ , we make use of the following theorem [58].

174 **Theorem 3.1.** *The product of two pseudo-differential operators  $A(\mathbf{x}, D) \in \Psi^{m_1}$  and  $B(\mathbf{x}, D) \in \Psi^{m_2}$  with symbols*  
 175  *$a(\mathbf{x}, \xi) \in S^{m_1}$  and  $b(\mathbf{x}, \xi) \in S^{m_2}$  respectively, is a composition operator  $C(\mathbf{x}, D) = A(\mathbf{x}, D)B(\mathbf{x}, D) \in \Psi^{m_1+m_2}$  with a*  
 176 *symbol  $c(\mathbf{x}, \xi) \in S^{m_1+m_2}$  having the asymptotic expansion given by*

$$c(\mathbf{x}, \xi) \sim \sum_{|\alpha| \leq N} \frac{1}{\alpha!} D_\xi^\alpha a(\mathbf{x}, \xi) \partial_x^\alpha b(\mathbf{x}, \xi) \quad (55)$$

177 for every nonnegative integer  $N$  and with the standard multi-index notation  $\alpha = (\alpha_1, \alpha_2, \dots, \alpha_k)$ ,  $|\alpha| = \alpha_1 + \alpha_2 + \dots + \alpha_k$ ,  
 178  $\mathbf{x} = (x_1, x_2, \dots, x_k)$ ,  $\xi = (\xi_1, \xi_2, \dots, \xi_k)$ ,  $D^\alpha = D^{\alpha_1} D^{\alpha_2} \dots D^{\alpha_k}$  and  $\partial^\alpha = \partial^{\alpha_1} \partial^{\alpha_2} \dots \partial^{\alpha_k}$ . Thus, the symbol  $c := ab$  of the  
 179 product of the pseudo-differential operators  $A(x, t, D_t)$  and  $B(x, t, D_t)$  is asymptotic to

$$c(x, t, \tau) \sim \sum_{k, l, n \geq 0} \frac{(-i)^n}{n!} \partial_\tau^n a_{1-k}(x, t, \tau) \partial_t^n b_{1-l}(x, t, \tau). \quad (56)$$

180 Substitution of (54) and (56) in (53) and casting-out  $R$  lead to

$$\begin{aligned} v^2(i\tau)^2 - \beta(i\tau)\partial_x^2 - 2\gamma u_t^{(0)}(i\tau) &= \sum_{j \geq 0} (a_{1-j} + b_{1-j})\partial_x + \sum_{j \geq 0} \partial_x b_{1-j} \\ &- \sum_{j \geq 0, k+l+n=j} \underbrace{\left( \frac{(-i)^n}{n!} \partial_\tau^n a_{1-k} \partial_t^n b_{1-l} \right)}_{O(\tau^{2-j})}, \quad k, l, n \geq 0. \end{aligned} \quad (57)$$

181 By equating the symbols with the same degree of homogeneity on both sides of equation (57) we can find the  
 182 coefficients  $a_{1-j}$  and  $b_{1-j}$  for  $j \geq 0$ . Typically, the more coefficients are taken the more accurate ABCs are. However,  
 183 taking more coefficients also makes the ABCs more complicated and involved to implement, since they contain higher  
 184 order derivatives. Therefore, we only show how to find the coefficients  $\{a_j, b_j\}_{j=\{1,0,-1\}}$  and note that other coefficients  
 185 can be calculated analogously. In order to define the first pair of coefficients  $a_1$  and  $b_1$ , we equate the symbols with  
 186 the degree of homogeneity  $O(\tau^2)$ . This gives the system of equations

$$\begin{cases} a_1 + b_1 = 0, \\ v^2(i\tau)^2 = -a_1 b_1. \end{cases} \quad (58)$$

187 To make the terms of order  $O(\tau^2)$  vanish we took the following solution to (58)

$$b_1 = -a_1 = v(i\tau). \quad (59)$$

188 **Remark 3.1.** *The choice of the sign in front of  $v(i\tau)$  is not arbitrary, since it defines the propagation direction of the*  
 189 *wave.*



190 In order to find the next pair of coefficients  $a_0, b_0$  we equate the symbols with degree of homogeneity  $\mathcal{O}(\tau^1)$  that  
 191 gives the following system of equations

$$\begin{cases} a_0 + b_0 = 0, \\ \beta(i\tau)\partial_x^2 + 2\gamma u_t^{(0)}(i\tau) = a_1 b_0 + a_0 b_1 - ia_{1\tau} b_{1t} - b_{1x}, \end{cases} \quad (60)$$

192 in terms of unknowns  $a_0, b_0$ .

193 Substitution of  $b_1 = -a_1$  in (60) yields

$$b_0 = -a_0 = -\frac{1}{2a_1} \left( ia_{1\tau} a_{1t} + a_{1x} - \beta(i\tau)\partial_x^2 - 2\gamma u_t^{(0)}(i\tau) \right) \quad (61)$$

194 or, in terms of  $a_1 = -v(i\tau)$ , we have

$$b_0 = -a_0 = -\frac{1}{2v} \left( \mathcal{A}_0[v] + \beta\partial_x^2 + 2\gamma u_t^{(0)} \right) \quad (62)$$

195 with the operator  $\mathcal{A}_0 := \partial_x + v\partial_t$ .

196 **Remark 3.2.** Note that here we exchanged the order of  $b_0$  and  $a_1$ . However, with  $a_1, b_0, a_0$  as above this is obviously  
 197 not correct as long as  $\beta \neq 0$  since, for example, in  $a_0 b_1$  the second order space derivative from  $a_0$  acts on the function  
 198  $v$  from  $b_1$ . These difficulties are caused by the strong damping term  $\beta\Delta u$  in deriving ABCs, and have a quite natural  
 199 explanation: The strong damping term destroys the wave like character of the equation since it implies decay of the  
 200 energy and a rather parabolic than hyperbolic behaviour of the equation, cf. [37]. Moreover, note that the  $\beta$  term  
 201 would lead to a second order normal derivative term in the first order and even to a fourth order normal derivative  
 202 term in the second order absorbing boundary conditions. Vanishing  $\beta$  enables us to recover commutativity of the  
 203 operators  $a_1$  and  $b_0$  as required to justify the derivations above. In the following we omit the term with  $\beta$  in (62) i.e.  
 204 consider

$$b_0 = -a_0 = -\frac{1}{2v} \left( \mathcal{A}_0[v] + 2\gamma u_t^{(0)} \right) \quad (63)$$

205 instead, and also set  $\beta = 0$  in the further derivation of absorbing boundary conditions.

206 In order to obtain more accurate boundary conditions we equate the symbols with degree of homogeneity  $\mathcal{O}(\tau^0)$ ,  
 207 which leads to the following system of equations

$$\begin{cases} a_{-1} + b_{-1} = 0, \\ -a_1 b_{-1} - a_0 b_0 - a_{-1} b_1 + i(a_{1\tau} b_{0t} + a_{0\tau} b_{1t}) - \frac{i^2}{2} a_{1\tau\tau} b_{1tt} + b_{0x} = 0. \end{cases} \quad (64)$$

208 The solution to (64) is given by

$$b_{-1} = -a_{-1} = -\frac{1}{2a_1} \left( -a_0^2 + i(a_{1\tau} a_{0t} + a_{0\tau} a_{1t}) + \frac{1}{2} a_{1\tau\tau} a_{1tt} + a_{0x} \right). \quad (65)$$

209 Taking into account (59) and (62) we deduce that

$$b_{-1} = -a_{-1} = \frac{1}{2v(i\tau)} \left( \mathcal{A}_0 \left[ \frac{1}{2v} \left( \mathcal{A}_0[v] + 2\gamma u_t^{(0)} \right) \right] - \left( \frac{1}{2v} \left( \mathcal{A}_0[v] + 2\gamma u_t^{(0)} \right) \right)^2 \right) =: \frac{\gamma\mu}{2v(i\tau)}. \quad (66)$$

210 Again we have exchanged the order of the operators to have  $a_1 b_{-1} + a_{-1} b_1 = a_1 b_{-1} - a_{-1} a_1 = a_1(b_{-1} - a_{-1})$ . Having  
 211 set  $\beta = 0$  helps here as well, since this renders  $a_{-1}(x, t, D_t)D_t$  a plain multiplication operator. Note that with the  
 212 Taylor linearization (47) an offset term  $\gamma(u^{(0)2})_{tt}$  would have appeared here, which would have prevented the equality  
 213  $a_{-1} a_1 = a_1 a_{-1}$ . (Here, we write  $f$  for the symbol of the zero order differential operator  $u \mapsto f$  (constant mapping),  
 214 which has to be strictly distinguished from the multiplication operator  $u \mapsto f \cdot u$ .) This problem is avoided by using the  
 215 fixed point type linearization (46).

216 According to [43], the operator

$$\partial_x - a(x, t, D_t) = 0 \tag{67}$$

217 annihilates outgoing waves at  $\{x = 0\} \times (0, T)$  and thus can be used to construct ABCs of different orders of accuracy.  
 218 Substitution of the asymptotic expansion (54a) with the first  $k$  leading terms into (67) results in the following boundary  
 219 condition

$$\left( \partial_x - \sum_{j=0}^k a_{1-j}(x, t, D_t) \right) u \Big|_{x=0} = 0. \tag{68}$$

220 An ABC of order  $k$  can be obtained from (68) by keeping the first  $k$  terms.

221 Thus, in order to construct a zero order ABC we set  $k = 0$  and substitute the coefficient  $a_1$  in (68), which gives

$$\mathcal{A}_0[u] \Big|_{x=0} = (u_x + \nu u_t) \Big|_{x=0} = 0. \tag{69}$$

222 Parallel to the construction of the zero order ABC (69), we set  $k = 1$  and substitute  $a_1, a_0$  in (68) to obtain the first  
 223 order boundary condition:

$$\mathcal{A}_1 u \Big|_{x=0} = (\mathcal{A}_0 - \mathcal{B}_1) u \Big|_{x=0} = \left( u_x + \nu u_t - \frac{1}{2\nu} \left( (\nu_x + \nu \nu_t) u + 2\gamma u_t^{(0)} u \right) \right) \Big|_{x=0} = 0 \tag{70}$$

224 with  $\mathcal{B}_1 := \frac{1}{2\nu} (\mathcal{A}_0[v] + 2\gamma u_t^{(0)})$ .

225 For  $k = 2$  we obtained the second order ABC

$$\mathcal{A}_2 u \Big|_{x=0} = (\mathcal{A}_1 u_t - \mathcal{B}_2 u) \Big|_{x=0} = \left( u_{xt} + \nu u_{tt} - \frac{1}{2\nu} \left( (\nu_x + \nu \nu_t) u_t + 2\gamma u_t^{(0)} u_t - \mu u \right) \right) \Big|_{x=0} = 0, \tag{71}$$

226 where we multiplied with  $(i\tau)$  before converting from symbols to operators, and where  $\mathcal{B}_2 := \frac{\gamma \mu(u^{(0)})}{2\nu(u^{(0)})}$  with

$$\begin{aligned} \mu(v) &= \frac{1}{\gamma} \mathcal{A}_0 \left[ \frac{1}{2\nu(v)} (\mathcal{A}_0[v(v)] + 2\gamma \nu_t) \right] - \left( \frac{1}{2\nu(v)} (\mathcal{A}_0[v(v)] + 2\gamma \nu_t) \right)^2 \\ &= \mathcal{A}_0 \left[ \frac{1}{2\sqrt{c^{-2} - 2\gamma v}} \left( -\frac{\nu_x}{\sqrt{c^{-2} - 2\gamma v}} + \nu_t \right) \right] - \gamma \left( \frac{1}{2\sqrt{c^{-2} - 2\gamma v}} \left( -\frac{\nu_x}{\sqrt{c^{-2} - 2\gamma v}} + \nu_t \right) \right)^2. \end{aligned} \tag{72}$$

227 Inserting  $u$  itself for the a priori solution  $u^{(0)}$ , we arrive at zero

$$\left( u_x + \sqrt{c^{-2} - 2\gamma u} u_t \right) \Big|_{x=0} = 0, \tag{73}$$

228 first

$$\left( u_x + \sqrt{c^{-2} - 2\gamma u} u_t - \frac{\gamma}{2\sqrt{c^{-2} - 2\gamma u}} \left( u_t u - \frac{1}{\sqrt{c^{-2} - 2\gamma u}} u_x u \right) \right) \Big|_{x=0} = 0, \tag{74}$$

229 and second order

$$\left( u_{xt} + \sqrt{c^{-2} - 2\gamma u} u_{tt} - \frac{\gamma}{2\sqrt{c^{-2} - 2\gamma u}} \left( (u_t)^2 - \frac{1}{\sqrt{c^{-2} - 2\gamma u}} u_x u_t - \mu(u) u \right) \right) \Big|_{x=0} = 0 \tag{75}$$

230 nonlinear ABCs for the Westervelt equation (48). Note that slightly different boundary conditions result from the  
 231 derivation via the para-differential approach presented in Section 3.2.

232 3.2. Absorbing boundary conditions in 1-d via para-differential calculus

233 In this part, we focus on the construction of absorbing boundary conditions for the Westervelt equation (43) with no  
 234 preliminary linearization in contrast to the approach used in Section 3.1. The disadvantage of the pseudo-differential  
 235 approach for designing ABCs is in its inability to treat nonlinear equations. This obstacle can be overcome by using the  
 236 para-differential calculus originated from the paper of Bony [36] with an improvement done by Meyer [44]. Although  
 237 the para-differential calculus and especially Bony’s para-linearization technique embrace wide opportunities to build  
 238 ABCs for nonlinear equations, their use is still very restricted in current research works. The first application of para-  
 239 differential operators to the development of ABCs has been done for the Burgers equation in [18]. Some relatively  
 240 recent results can be found in few works (e.g. [52, 51]).

241 Before the derivation of ABCs we briefly recall some general facts about para-differential operators and Bony’s  
 242 para-linearization. Let us consider a nonlinear differential equation of order  $N$  defined as follows

$$F[u](x) = \Phi(x, u(x), \dots, \partial^\alpha u(x), \dots)_{0 \leq |\alpha| \leq N} = 0 \tag{76}$$

243 with  $\Phi \in C^\infty$  and  $x \in \mathbb{R}^d$ . In accordance to [36], the para-linearization of (76) with  $\Phi(x, \cdot)$  vanishing at 0 is given by

$$F[u] = \sum_{0 \leq |\alpha| \leq N} T_{F'(u)} \partial^\alpha u + R(u), \tag{77}$$

244 where  $T_{F'(u)}$  is a para-differential operator having as symbol the linearization  $F'(u) = \frac{\partial \Phi}{\partial \lambda_\alpha}(\cdot, u, \dots, \partial^\alpha u, \dots)_{0 \leq |\alpha| \leq N}$  of  $F$   
 245 at  $u$ , and  $R(u)$  is a smooth error. More precisely, for all  $u \in H^s(\mathbb{R}^d)$  with  $s > d/2$  equation (77) implies  $R(u) \in H^{2s-d/2}$   
 246 (see [44]). Equation (77) is often referred to as the para-linearization formula of Bony, and the para-differential  
 247 operator  $T_a$  with a symbol  $a(x) \in C^\infty$ ,  $x \in \mathbb{R}^d$  is defined as

$$\mathcal{F}(T_a u)(\zeta) = \frac{1}{(2\pi)^d} \int_{\mathbb{R}^d} \chi(\zeta - \eta, \eta) \mathcal{F} a(\zeta - \eta) \mathcal{F} u(\eta) d\eta, \tag{78}$$

248 where  $\mathcal{F}$  is the Fourier transform, and  $\chi \in C^\infty(\mathbb{R}^d \times \{\mathbb{R}^d \setminus \{0\}\})$  is a function of homogeneity degree zero satisfying

$$\begin{cases} \chi(\zeta, \eta) = 1 & \text{if } |\zeta| \leq \varepsilon_1 |\eta|, \\ \chi(\zeta, \eta) = 0 & \text{if } |\zeta| \geq \varepsilon_2 |\eta|, \end{cases} \tag{79}$$

249 with  $0 < \varepsilon_1 < \varepsilon_2$ .

250 Before the derivation of ABCs for the Westervelt equation (48), we develop the nonlinear term on its right hand  
 251 side  $\gamma(u^2)_{tt} = 2\gamma((u_t)^2 + uu_{tt})$  and recast (48) in the form

$$v^2(u)u_{tt} - u_{xx} - \beta u_{txx} = 2\gamma(u_t)^2 \tag{80}$$

252 with  $v^2(u) = c^{-2} - 2\gamma u$ .

253 Based on (77) and taking into account that the product of two functions  $f$  and  $g$  can be written in term of para-  
 254 differential operators [36] as

$$fg = T_f g + T_g f + R, \tag{81}$$

255 where  $T_f$  and  $T_g$  are para-differential operators with symbols  $f$  and  $g$ , we obtain the para-linearized Westervelt equa-  
 256 tion in the operator form

$$\mathfrak{D}_2 u = 0, \quad \mathfrak{D}_2 = c^{-2} \partial_t^2 - 2\gamma(T_{u_{tt}} + T_u \partial_t^2) - \partial_x^2 - \beta \partial_{txx} - 2\gamma T_{2u_t} \partial_t \tag{82}$$

257 instead of the Westervelt equation (80).

258 Acting similar to the previous derivation, we apply Nirenberg’s factorization, analogous to (51), and rewrite (82)  
 259 in the form

$$\mathfrak{D}_2 = -(\partial_x - A)(\partial_x - B) + R, \tag{83}$$

260 where  $A$  and  $B$  are para-differential operators with symbols  $a$  and  $b$ , respectively.

261 A similar argument as for the linearized Westervelt equation yields

$$v^2(u)(i\tau)^2 - 2\gamma u_{tt} - \beta(i\tau)\partial_x^2 - 4\gamma u_t(i\tau) = (a + b)\partial_x + \partial_x b - ab + R. \quad (84)$$

262 Note that this equation differs from (53) and also leads to different ABCs. Again, we skip the  $\beta$  terms for the same  
263 reason as in Section 3.1.

264 Substitution of asymptotic expansions of symbols (54) and (55) in (84) results in equation (57) from which, by  
265 equating the symbols of the same degree of homogeneity  $O(\tau^2)$  on both sides, we obtain the same coefficients

$$b_1 = -a_1 = v(i\tau). \quad (85)$$

266 However, the equation for the  $O(\tau^1)$  terms is different compared to (60), namely

$$\begin{cases} a_0 + b_0 = 0, \\ \beta(i\tau)\partial_x^2 + 4\gamma u_t^{(0)}(i\tau) = a_1 b_0 + a_0 b_1 - ia_{1\tau} b_{1t} - b_{1x}, \end{cases} \quad (86)$$

267 which upon setting  $\beta = 0$  yields (as opposed to (63))

$$b_0 = -a_0 = -\frac{1}{2v} (\mathcal{A}_0[v] + 4\gamma u_t) \quad (87)$$

268 with the operator  $\mathcal{A}_0 := \partial_x + v\partial_t$ .

269 Finally, in contrast to (64), we have the following equation for the  $O(\tau^0)$  terms

$$\begin{cases} a_{-1} + b_{-1} = 0, \\ -a_1 b_{-1} - a_0 b_0 - a_{-1} b_1 + i(a_{1\tau} b_{0t} + a_{0\tau} b_{1t}) - \frac{i^2}{2} a_{1\tau\tau} b_{1tt} + b_{0x} = -2\gamma u_{tt}, \end{cases} \quad (88)$$

270 so that we get

$$b_{-1} = -a_{-1} = \frac{1}{2v(i\tau)} \left( \mathcal{A}_0 \left[ \frac{1}{2v} (\mathcal{A}_0[v] + 4\gamma u_t) \right] - \left( \frac{1}{2v} (\mathcal{A}_0[v] + 4\gamma u_t) \right)^2 - 2\gamma u_{tt} \right) =: \frac{\tilde{\mu}}{2v(i\tau)}. \quad (89)$$

271 Parallel to the ABCs for the linearized Westervelt equation from Section 3.1, we obtained the zero order ABC

$$\mathcal{A}'_0 u|_{x=0} = (\partial_x + v(u)\partial_t) u|_{x=0} = 0, \quad (90)$$

272 the first order one

$$\mathcal{A}'_1 u|_{x=0} = (\mathcal{A}'_0 - \mathcal{B}'_1) u|_{x=0} = \left( \partial_x + v(u)\partial_t - \frac{1}{2v(u)} (\mathcal{A}'_0[v(u)] + 4\gamma u_t) \right) u|_{x=0} = 0, \quad (91)$$

273 with  $\mathcal{B}'_1 := \frac{1}{2v(u)} (\mathcal{A}'_0[v] + 4\gamma u_t)$ , and the second order boundary condition

$$\mathcal{A}'_2 u|_{x=0} = (\mathcal{A}'_1 u_t - \mathcal{B}'_2 u)|_{x=0} = \left( u_{xt} + v u_{tt} - \frac{1}{2v} ((v_x + v v_t) u_t + 4\gamma (u_t)^2 - \tilde{\mu} u) \right) \Big|_{x=0} = 0, \quad (92)$$

274 where  $\mathcal{B}'_2 := \tilde{\mu}(u)$ , which contains multiplication with  $u_{tt}$ , as opposed to (71). As in the pseudo-differential case, we  
275 do not consider higher order boundary conditions, although their derivation follows the same lines.

### 276 3.3. Absorbing boundary conditions in 1-d via asymptotic expansions

277 An alternative approach to the derivation of ABCs for the Westervelt equation (48) can be based on the asymptotic  
278 expansion of the solution  $u(x, t)$  in an  $\varepsilon$ -neighborhood of  $u^{(0)}(x, t)$  in terms of  $\varepsilon$ , namely

$$u = u^{(0)} + \varepsilon u^{(1)} + \varepsilon^2 u^{(2)} + \dots \quad (93)$$

279 For the purposes pursued in this work it is enough to consider the terms of order  $\varepsilon$  in (93). Plugging (93), up to the  
 280 terms  $\mathcal{O}(\varepsilon^1)$ , into (48) gives

$$c^{-2}(u^{(0)} + \varepsilon u^{(1)})_{tt} - (u^{(0)} + \varepsilon u^{(1)})_{xx} - \beta(u^{(0)} + \varepsilon u^{(1)})_{txx} = \gamma(u^{(0)2} + 2\varepsilon u^{(0)}u^{(1)} + \varepsilon^2 u^{(1)2})_{tt}. \quad (94)$$

281 The standard asymptotic argument implies equating the terms of the same degree in  $\varepsilon$ . In particular, for  $\mathcal{O}(\varepsilon^0)$  we  
 282 have

$$c^{-2}u_{tt}^{(0)} - u_{xx}^{(0)} - \beta u_{txx}^{(0)} = \gamma(u^{(0)2})_{tt}. \quad (95)$$

283 Equation (95) is satisfied for  $u^{(0)}$ , since this is the solution to equation (48).

284 By equating the terms of order  $\varepsilon$ , we obtain the linearized Westervelt equation

$$c^{-2}u_{tt}^{(1)} - u_{xx}^{(1)} - \beta u_{txx}^{(1)} = 2\gamma(u^{(0)}u^{(1)})_{tt}$$

285 or alternatively in the operator form, with replacing  $u^{(1)}$  for  $u$ ,

$$\widetilde{\mathcal{D}}_1 u = 0, \quad \widetilde{\mathcal{D}}_1 = v^2 \partial_t^2 - \partial_x^2 - \beta \partial_{txx} - 2\gamma(u^{(0)} \text{id} + 2u_t^{(0)} \partial_t). \quad (96)$$

286 As can be seen, equations (82) and (96) are exactly the same equations at the symbolic level, thereby eventually  
 287 leading to the same ABCs. Thus, the para-differential approach to the construction of ABCs is equivalent to the  
 288 asymptotic expansion method.

289 In order to para-linearize the Westervelt equation the para-differential approach uses the Taylor expansion with  
 290 the assumption that the nonlinear function vanishes at zero. This means that in terms of the Taylor linearization of the  
 291 right hand side  $f(u) = \gamma(u^2)_{tt}$  of the Westervelt equation (43),  $f(u)$  vanishes at the reference solution  $u^{(0)}$ . Therefore,  
 292 the following remark is valid.

293 **Remark 3.3.** *The same assumption, the para-differential technique relies on, being introduced into the Taylor expansion  
 294 applied to the right hand side of the Westervelt equation (43) gives the same result as the para-linearization thus  
 295 making these approaches equivalent to each other. From the other hand, the para-linearization is equivalent to the  
 296 asymptotic expansion as well as to the Taylor linearization, which, as we showed, prevents the offset term  $\gamma\left(\left(u^{(0)}\right)^2\right)_{tt}$   
 297 of being introduced into the absorbing boundary conditions. Therefore, we conclude that there do not appear to be  
 298 sufficient reasons to derive ABCs through the para-differential technique unless the coefficients have limited regularity.*

299 Overall, we found that the para-differential technique is equivalent to both the asymptotic expansion of the West-  
 300 ervelt equation and to the linearization of its right hand side through the standard linearization according to the first  
 301 order Taylor expansion with the assumption that the nonlinear function vanishes at the reference solution  $u^{(0)}$ .

### 302 3.4. Absorbing boundary conditions in 2-d via linearization and pseudo-differential calculus

303 In the spatially two dimensional situation the operator form of the Westervelt equation (43) reads as

$$\mathcal{D}_1 u = 0, \quad \text{with } \mathcal{D}_1 = v^2 \partial_t^2 - \partial_x^2 - \partial_y^2 - \beta \partial_{txx} - \beta \partial_{tyy} - 2\gamma u_t^{(0)} \partial_t \quad \text{in } (-\infty, 0) \times \mathbb{R}, \quad (97)$$

304 where  $v$  is defined by (50). Here, we proceed very similarly to the 1-d case, and consider pseudo-differential operators  
 305  $A = A(x, y, t, D_y, D_t)$  and  $B = B(x, y, t, D_y, D_t)$  with respect to time and tangential (i.e.  $y$ ) direction, but the expansion  
 306 is still with respect to powers of  $\tau$ , so equations (51), (52) (with  $A = A(x, y, t, D_y, D_t)$  and  $B = B(x, y, t, D_y, D_t)$ ) remain  
 307 the same, whereas (53), (54), (57) change to

$$v^2(i\tau)^2 - (i\eta)^2 - \beta(i\tau)\partial_x^2 - \beta(i\tau)(i\eta)^2 - 2\gamma u_t^{(0)}(i\tau) = (a + b)\partial_x + b_x - ab + R \quad (98)$$

308 with the correspondence  $i\eta \leftrightarrow \partial_y$  and

$$a(x, y, t, \eta, \tau) \sim \sum_{j \geq 0} a_{1-j}(x, y, t, \eta, \tau), \quad |\tau| \rightarrow \infty, \quad (99a)$$

309 
$$b(x, y, t, \eta, \tau) \sim \sum_{j \geq 0} b_{1-j}(x, y, t, \eta, \tau), \quad |\tau| \rightarrow \infty, \quad (99b)$$

310 and

$$\begin{aligned} v^2(i\tau)^2 - (i\eta)^2 - \beta(i\tau)\partial_x^2 - \beta(i\tau)(i\eta)^2 - 2\gamma u_t^{(0)}(i\tau) &= \sum_{j \geq 0} (a_{1-j} + b_{1-j})\partial_x + \sum_{j \geq 0} \partial_x b_{1-j} \\ &- \sum_{j \geq 0, k+l+n=j} \underbrace{\left( \frac{(-i)^n}{n!} \partial_\tau^n a_{1-k} \partial_t^n b_{1-l} \right)}_{O(\tau^{2-l})}, \quad k, l, n \geq 0, \end{aligned} \quad (100)$$

311 respectively, where  $a_{1-j}$  and  $b_{1-j}$  are homogeneous functions of degree  $1 - j$  in  $\tau$  (and are additionally functions of  
312  $x, y, t$ , and  $\eta$ ). As in [19], in our derivations we rely on an assumption of the type  $\eta \sim \tau$ . Therewith,  $\beta(i\tau)(i\eta)^2$  becomes  
313 a third order term that cannot be matched by the right hand side. Thus, in two space dimensions we already here  
314 arrived at the limitations due to the strong damping term (see also Remark 3.2 above), which we therefore omitted  
315 from now on by setting  $\beta = 0$ . Considering the  $O(\tau^2)$  terms in (100) leads to

$$\begin{cases} v^2(i\tau)^2 - (i\eta)^2 = -a_1 b_1, \\ a_1 + b_1 = 0. \end{cases} \quad (101)$$

316 in place of (58), which results in

$$b_1 = -a_1 = \sqrt{v^2(i\tau)^2 - (i\eta)^2}. \quad (102)$$

317 At this point, a fundamental difference to the 1-d case arises, since one has to approximate the square root

$$\sqrt{v^2(i\tau)^2 - (i\eta)^2} = v(i\tau) \sqrt{1 - \frac{\eta^2}{v^2\tau^2}}$$

318 in order to derive practically applicable boundary conditions. We do so by a Taylor expansion whose order is adapted  
319 to the order of the ABCs.

320 The calculations for  $a_0, b_0$  look exactly the same as in the 1-d case and yield

$$b_0 = -a_0 = -\frac{1}{2a_1} (ia_{1\tau}a_{1t} + a_{1x} - 2\gamma u_t^{(0)}(i\tau)) \quad (103)$$

321 i.e.

$$b_0 = -a_0 = -\frac{v_t}{2} \left(1 - \frac{\eta^2}{v^2\tau^2}\right)^{-3/2} - \frac{v_x}{2v} \left(1 - \frac{\eta^2}{v^2\tau^2}\right)^{-1} - \frac{2\gamma u_t^{(0)}}{2v} \left(1 - \frac{\eta^2}{v^2\tau^2}\right)^{-1/2}. \quad (104)$$

322 To obtain zero order boundary condition we use the zero order Taylor expansion

$$(1 - x)^{1/2} \approx 1, \quad x := \frac{\eta^2}{v^2\tau^2}$$

323 in (102) to have

$$\tilde{b}_1^0 = -\tilde{a}_1^0 = v(i\tau). \quad (105)$$

324 For our first order boundary condition we use the first order Taylor approximation

$$(1 - x)^{1/2} \approx 1 - \frac{1}{2}x, \quad (1 - x)^{-3/2} \approx 1 + \frac{3}{2}x, \quad (1 - x)^{-1} \approx 1 + x, \quad (1 - x)^{-1/2} \approx 1 + \frac{1}{2}x$$

325 for the terms that are nonlinear with respect to  $\tau, \eta$  in (103) and (104). This yields the following symbols

$$\begin{aligned} \tilde{b}_1^1 = -\tilde{a}_1^1 &= v(i\tau) \left(1 - \frac{\eta^2}{2v^2\tau^2}\right), \\ \tilde{b}_0^1 = -\tilde{a}_0^1 &= -\frac{v_t}{2} \left(1 + \frac{3\eta^2}{2v^2\tau^2}\right) - \frac{v_x}{2v} \left(1 + \frac{\eta^2}{v^2\tau^2}\right) - \frac{2\gamma u_t^{(0)}}{2v} \left(1 + \frac{\eta^2}{2v^2\tau^2}\right). \end{aligned}$$

326 Again we insert  $u$  itself for the a priori solution  $u^{(0)}$  to arrive at the zero order ABC

$$\left( u_x + \sqrt{c^{-2} - 2\gamma u} u_t \right) \Big|_{x=0} = 0 \quad (106)$$

327 and at the first order boundary condition

$$\begin{aligned} & \left( u_{xt} + \sqrt{c^{-2} - 2\gamma u} u_{tt} - \frac{1}{2\sqrt{c^{-2} - 2\gamma u}} u_{yy} - \frac{\gamma}{2\sqrt{c^{-2} - 2\gamma u}} \left( u_t - \frac{1}{\sqrt{c^{-2} - 2\gamma u}} u_x \right) u_t \right. \\ & \left. + \frac{\gamma}{2(c^{-2} - 2\gamma u)^{3/2}} \left( \frac{1}{2} u_t + \frac{1}{\sqrt{c^{-2} - 2\gamma u}} u_x \right) \int_0^t u_{yy} dt \right) \Big|_{x=0} = 0, \end{aligned} \quad (107)$$

328 where we have multiplied the symbols with  $(i\tau)$  to obtain (107) or alternatively

$$\begin{aligned} & \left( u_{xtt} + \sqrt{c^{-2} - 2\gamma u} u_{ttt} - \frac{1}{2\sqrt{c^{-2} - 2\gamma u}} u_{yyt} \right. \\ & \left. - \frac{\gamma}{2\sqrt{c^{-2} - 2\gamma u}} \left( u_t - \frac{1}{\sqrt{c^{-2} - 2\gamma u}} u_x \right) u_{tt} + \frac{\gamma}{2(c^{-2} - 2\gamma u)^{3/2}} \left( \frac{1}{2} u_t + \frac{1}{\sqrt{c^{-2} - 2\gamma u}} u_x \right) u_{yy} \right) \Big|_{x=0} = 0, \end{aligned} \quad (108)$$

329 where we have multiplied the symbols with  $(i\tau)^2$  to obtain (108).

#### 330 4. Discretization

331 In this section we consider the space and time discretizations for problem (43)-(45) and how to couple the derived  
332 ABCs with the numerical methods used. Our focus is on the 2-d ABCs, since the 1-d boundary conditions use the  
333 same principle for coupling. For the space discretization we apply the finite element method with the standard setting  
334 of Sobolev spaces for evolution problems, while the time integration is done by the classical Newmark method.

335 For the weak formulation it is natural to use the space  $H^1$ , then the resulting variational problem reads as follows:  
336 for given initial data  $u(\cdot, t = 0) = u_0$ ,  $u_t(\cdot, t = 0) = u_1$ , find  $u \in L^2(0, T; H^1(\Omega))$ ,  $u_t \in L^2(0, T; L^2(\Omega))$  and  $u_{tt} \in$   
337  $L^2(0, T; H^{-1}(\Omega))$  such that for all  $\phi \in H^1$  and for all times  $t \in (0, T)$

$$\langle c^{-2} u_{tt}, \phi \rangle_{\Omega} + (\nabla u, \nabla \phi)_{\Omega} - (u_n + \beta u_m, \phi)_{\Gamma_A} - (\beta \nabla u_t, \nabla \phi)_{\Omega} - (\gamma (u^2)_{tt}, \phi)_{\Omega} = (g(t) + \beta u_m, \phi)_{\Gamma_N} \quad (109)$$

338 with  $\langle \cdot, \cdot \rangle_{\Omega}$  denoting the duality product on  $H^1(\Omega) \times H^{-1}(\Omega)$  and  $(\cdot, \cdot)$  standing for  $L^2$ -inner product.

339 The integration of the zero order ABC (106) into the weak formulation (109) is straightforward: one has to express  
340 the ABC in terms of  $u_n$  and substitute it into the boundary term

$$-(u_n + \beta u_m, \phi)_{\Gamma_A}, \quad (110)$$

341 which gives

$$(\nu(u) u_t + (\nu(u) u_t)_t, \phi)_{\Gamma_A}.$$

342 However, such a straightforward substitution is not applicable to the first order ABC (108). In this case, we use a  
343 Lagrange multiplier (LM) based approach proposed in [49]. The main idea is to introduce the LMs  $\lambda = -u_n$  and  
344  $\kappa = u_t$  on the absorbing boundary  $\Gamma_A$  and recast the boundary integral (110) as

$$-(u_n + \beta u_m, \phi)_{\Gamma_A} = (\lambda + \beta \lambda_t, \phi)_{\Gamma_A}, \quad (\lambda, \phi)_{\Gamma_A} := \int_{\Gamma_A} \lambda \phi \, d\Gamma_A = \sum_{i=1}^l \int_{\Gamma_A^i} \lambda \phi \, d\Gamma_A^i, \quad (111)$$

345 where  $\Gamma_A$  is assumed to be piecewise smooth and decomposed into  $l$  non-overlapping smooth subparts  $\Gamma_A^i$ .

346 To couple the first order boundary condition (108) and equation (109) we reformulate (108) in the weak form:

$$-(\lambda_{tt}, \mu)_{\Gamma_A^i} + (v(u)\kappa_{tt}, \mu)_{\Gamma_A^i} - \frac{\kappa_\tau \mu}{2\nu} \Big|_{\partial\Gamma_A^i} + \left( \kappa_\tau, \left( \frac{\mu}{2\nu} \right)_\tau \right)_{\Gamma_A^i} - \left( \frac{\gamma\kappa_t}{2\nu} \left( \kappa + \frac{\lambda}{\nu} \right), \mu \right)_{\Gamma_A^i} + \theta u_\tau \mu \Big|_{\partial\Gamma_A^i} - (u_\tau \theta_\tau, \mu)_{\Gamma_A^i} = 0, \quad (112)$$

347 where  $\theta = \frac{\gamma}{2\nu^{3/4}} \left( \frac{\kappa}{2} - \frac{\lambda}{\nu} \right)$  and  $\tau$  is the tangential derivative to  $\Gamma_A^i$ , and  $\partial\Gamma_A^i$  denotes the endpoints of  $\Gamma_A^i$ ,  $i = 1, 2, \dots, l$ .

348 The boundary condition (112) holds for all test functions  $\mu$  out of an appropriate test space defined on  $\Gamma_A^i$ . To get  
349 rid of the terms on  $\partial\Gamma_A^i$ , we allow only for test functions  $\mu$  being equal to zero on  $\partial\Gamma_A^i$ ,  $i = 1, 2, \dots, L$ . Using for  $\mu$   
350 piecewise linear and continuous hat functions in  $H_0^1(\Gamma_A^i)$ , we end up with

$$-(\lambda_{tt}, \mu)_{\Gamma_A} + (v(u)\kappa_{tt}, \mu)_{\Gamma_A} + \left( \kappa_\tau, \left( \frac{\mu}{2\nu} \right)_\tau \right)_{\Gamma_A} - \left( \frac{\gamma\kappa_t}{2\nu} \left( \kappa + \frac{\lambda}{\nu} \right), \mu \right)_{\Gamma_A} - (u_\tau \theta_\tau, \mu)_{\Gamma_A} = 0. \quad (113)$$

351 To obtain a more simple algebraic structure, we use dual LMs [56, 57]. We also require no continuity for the LMs,  
352 since it would result in poor approximation properties. Thus, we apply the crosspoint modification of mortar finite  
353 elements to define the basis functions of the LMs ansatz space. With each interior node of  $\Gamma_A^i$  we associate one basis  
354 function. The ansatz space for the LMs differs from the test space for  $\mu$ , and we are formally in a Petrov–Galerkin  
355 setting. Note that by construction the dimension of the test and ansatz space is the same.

356 The algebraic formulation of the coupled problem (109), (113) can be expressed as a semi-discrete system of  
357 nonlinear ordinary differential equations

$$\mathcal{A}(\mathbf{v}^{n+1})\dot{\mathbf{v}}^{n+1} + \mathcal{B}(\mathbf{v}^{n+1})\mathbf{v}^{n+1} + \mathcal{C}(\mathbf{v}^{n+1})\mathbf{v}^{n+1} = \mathcal{F}^{n+1}, \quad (114)$$

358 with the vector of unknowns  $\mathbf{v} = (\mathbf{u}, \lambda, \kappa)^\top$  and the terms

$$\mathcal{A} = \begin{pmatrix} c^{-2}\mathbf{M} - 2\gamma\tilde{\mathbf{M}} & 0 & 0 \\ 0 & -\mathbf{D} & \tilde{\mathbf{B}} \\ 0 & 0 & 0 \end{pmatrix}, \quad \mathcal{B} = \begin{pmatrix} \beta\mathbf{K} - 2\gamma\tilde{\mathbf{M}} & \beta\mathbf{D}^\top & 0 \\ 0 & 0 & -\frac{\gamma}{2}\tilde{\mathbf{K}} \\ -\mathbf{M} & 0 & 0 \end{pmatrix}, \quad \mathcal{C} = \begin{pmatrix} \mathbf{K} & \mathbf{D}^\top & 0 \\ -\mathbf{P} & \mathbf{Q} & -\frac{\gamma}{2}\tilde{\mathbf{D}} \\ 0 & 0 & \mathbf{M} \end{pmatrix}, \quad \mathcal{F} = \begin{pmatrix} \mathbf{f} \\ \mathbf{0} \\ \mathbf{0} \end{pmatrix},$$

359 where the right hand side  $\mathbf{f}$  represents the Neumann boundary condition;  $\mathbf{M}$  and  $\mathbf{K}$  are the standard mass and stiffness  
360 matrices, respectively. The other matrices are responsible for nonlinear terms and coupling between the Westervelt  
361 equation and the ABC.

362 In order to approximate the system of equations (114) in time, the generalized  $\alpha$ -method [12] is applied:

$$\dot{\mathbf{v}}^{n+1} = a_1 \mathbf{v}^{n+1} - \hat{\mathbf{v}}^n, \quad \dot{\mathbf{v}}^{n+1} = a_2 \mathbf{v}^{n+1} - \hat{\mathbf{v}}^n, \quad \text{where} \quad (115)$$

$$\hat{\mathbf{v}}^n = a_1 \mathbf{v}^n + \frac{(1 - \hat{\alpha}_f)\hat{\gamma} - \hat{\beta}}{\hat{\beta}} \dot{\mathbf{v}}^n + \frac{(1 - \hat{\alpha}_f)(\hat{\gamma} - 2\hat{\beta})}{2\hat{\beta}} \Delta t \ddot{\mathbf{v}}^n, \quad \hat{\mathbf{v}}^n = a_2 \mathbf{v}^n + \frac{1 - \hat{\alpha}_m}{\hat{\beta}\Delta t} \dot{\mathbf{v}}^n + \frac{1 - \hat{\alpha}_m - 2\hat{\beta}}{2\hat{\beta}} \ddot{\mathbf{v}}^n$$

363 with the parameters  $a_1 = (1 - \hat{\alpha}_f)\hat{\gamma}/(\hat{\beta}\Delta t)$ ,  $a_2 = (1 - \hat{\alpha}_m)/(\hat{\beta}\Delta t^2)$ , and  $\Delta t$  is a time step. In all computations we set  
364  $\hat{\alpha}_m = \hat{\alpha}_f = 0$ ,  $\hat{\beta} = 0.25$ ,  $\hat{\gamma} = 0.5$ , which results in the standard Newmark scheme [35] the application of which  
365 to (114) yields

$$a_2 \mathcal{A}(\mathbf{v}^{n+1})\mathbf{v}^{n+1} + a_1 \mathcal{B}(\mathbf{v}^{n+1})\mathbf{v}^{n+1} + \mathcal{C}(\mathbf{v}^{n+1})\mathbf{v}^{n+1} = \mathcal{F}^{n+1} + \mathcal{A}(\mathbf{v}^{n+1})\hat{\mathbf{v}}^n + \mathcal{B}(\mathbf{v}^{n+1})\hat{\mathbf{v}}^n. \quad (116)$$

366 To solve the nonlinear system (116) we use the Newton method, demonstrating excellent convergence behavior  
367 and robustness with respect to the choice of governing parameters in (43), acoustic source settings and ABCs.

## 368 5. Numerical results

369 In this part, we study the performance of the proposed absorbing boundary conditions in one and two space  
370 dimensions for different regimes of wave propagation. First, we analyzed the accuracy of ABCs derived with the  
371 pseudo-differential and para-differential approaches in a one dimensional waveguide. Second, we considered a two  
372 dimensional, horizontal waveguide with an inclined, artificial lateral wall and studied how the accuracy of the solution



373 was influenced by the angle of incidence and the excitation frequency. Third, we carried out numerical experiments  
 374 for the High Intensity Focused Ultrasound (HIFU) problem with settings typical for thermal ablation of tumors in the  
 375 human liver and analyzed how intensively the solution was contaminated by reflected waves.

376 We denote the absorbing boundary conditions as  $ABC_n^{d,o}$ , where the superscripts  $d$  and  $o$  indicate the space di-  
 377 mension and the order of ABC, respectively, while the subscript  $n$  stands for the pseudo- (PS) or para-differential  
 378 (PR) calculus based ABC, or the Engquist–Majda (EM) boundary condition, respectively. Here, by Engquist–Majda  
 379 ABCs we mean those designed for the linear wave equation, so not taking into account the nonlinearity and the strong  
 380 damping in the Westervelt equation.

381 In order to compare different ABCs, a reference solution  $u^*$  was computed in the domain  $\Omega' \ni \Omega$ , which is  
 382 large enough to prevent the solution in the restricted domain  $\Omega$  from being polluted during the computations. Note  
 383 that  $u^*$  was computed for the same problem settings and physical parameters as  $u$  (the solution affected by reflected  
 384 waves) but in a larger computational domain. The studied ABCs were compared in terms of an  $l^2$ -norm relative error  
 385  $\delta(u^*, u) = \|u^* - u\|_2 / \|u^*\|_2$ , between the reference solution and the solution  $u$  distorted by reflected waves. We also  
 386 introduce a difference  $\tilde{\delta}(u^*, u) = u^* - u$ , which allows us to track reflected waves. In all numerical experiments the  
 387 number of finite elements per wavelength was set to be 50, and the time step was chosen in such a way as to have 20  
 388 time samples per time period for each of the frequencies  $\omega = \{25 \text{ kHz}, 50 \text{ kHz}, 100 \text{ kHz}, 1 \text{ MHz}\}$ . To induce a wave in  
 389 the domain, a monofrequency excitation of the form  $u_n = \sin(2\pi\omega t)$  was used. The simulation time  $t$  and the initial  
 390 acoustic pressure amplitude were normalized to unity. The physical parameters in all numerical tests correspond to  
 391 those of human liver [28, 15]:  $c = 1596 \text{ m} \cdot \text{s}^{-1}$ ,  $\rho = 1050 \text{ kg} \cdot \text{m}^{-3}$ ,  $B/A = 6.8$ ,  $b = 2\alpha c^3 / (2\pi\omega)^2$ , with the acoustic  
 392 absorption coefficient  $\alpha = 4.5 \text{ Np} \cdot \text{m}^{-1} \cdot \text{MHz}^{-1}$ .

### 393 5.1. ABC in 1-d

394 In this section, we compare  $ABC_n^{1,o}$ , with  $o = \{0, 1\}$ ,  $n = \{\text{PS}, \text{PR}, \text{EM}\}$  on a line segment  $\Omega \in [0, 16 \text{ cm}]$  and study  
 395 how the excitation frequency of the transducer influences the performance of the ABCs considered. The excitation  $u_n$   
 396 with one of the frequencies  $\omega = \{25, 50, 100\} \text{ kHz}$  was set at the point  $\Gamma_N = 0$ , while the ABC studied was prescribed  
 397 at the point  $\Gamma_A = 16 \text{ cm}$  (Fig. 1).

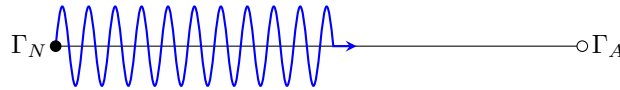
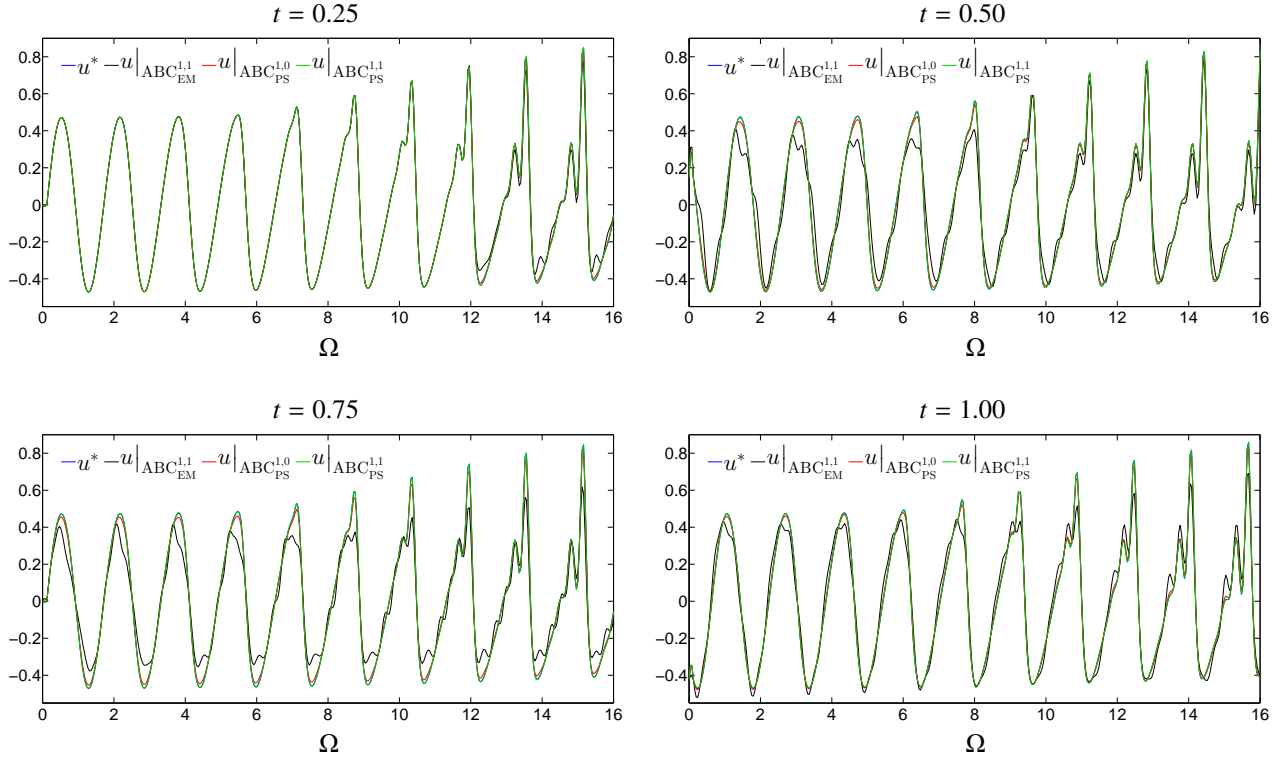


Fig. 1: General geometrical setup for the line segment domain  $\Omega$ .

398 We present a series of snapshots of the reference solution  $u^*$  and the solution  $u$  affected by the boundary conditions  
 399  $ABC_n^{1,o}$ ,  $o = \{0, 1\}$ ,  $n = \{\text{PS}, \text{EM}\}$  in Fig. 2. As can be seen, for  $t \in [0, 1]$ , the difference between  $ABC_{\text{PS}}^{1,0}$  and  $ABC_{\text{PS}}^{1,1}$  is  
 400 fairly small and slightly discloses itself only near the solution extrema. The same scenario is followed by the first order  
 401 Engquist–Majda condition but only for  $t \leq 0.2$ . However, as time advances the reflected waves start contaminating the  
 402 solution. More insightful information on how the boundary conditions perform in time is given by the relative error  $\delta$   
 403 presented in Fig. 3.

404 As can be seen from Fig. 3, the accuracy of the proposed ABCs does not significantly depend on the excitation  
 405 frequency, although the relative error  $\delta$  for the first order Engquist–Majda condition  $ABC_{\text{EM}}^{1,1}$  and the zero-order condi-  
 406 tion  $ABC_{\text{PS}}^{1,0}$  becomes somewhat higher in the low-frequency regimes. The first order conditions  $ABC_{\text{PS}}^{1,1}$  and  $ABC_{\text{PR}}^{1,1}$   
 407 perform equally well at all frequencies studied. The behaviour of the boundary conditions  $ABC_{\text{PS}}^{1,0}$  and  $ABC_{\text{PS}}^{1,1}$  brings  
 408 no surprise - the higher the order of the ABC is, the more accurate the solution becomes. The error  $\delta$ , introduced  
 409 by  $ABC_{\text{PS}}^{1,0}$ , exhibits a very moderate growth at the initial stage of the simulation ( $t \in [0.2, 0.6]$ ) with the maximum  
 410 reached at  $t \approx 0.6$ . For  $t > 0.6$ , the error moderately fluctuates around a mean value with no further growing. On the  
 411 other hand, the first order condition  $ABC_{\text{PS}}^{1,1}$  demonstrates qualitatively the same behaviour as the zero order one, but  
 412 on a much lower scale. The relative error  $\delta$  also fluctuates around a mean, but these fluctuations are much smaller  
 413 compared to those of  $ABC_{\text{PS}}^{1,0}$ . It is important to remark that the difference between  $ABC_{\text{PS}}^{1,1}$  and  $ABC_{\text{PR}}^{1,1}$  is virtually  
 414 the same, indicating that the additional term  $2\gamma u_t$  in  $ABC_{\text{PR}}^{1,1}$  (see the boundary condition (91) for detail) is of minor  
 415 importance. In contrast to the proposed ABCs, the first order Engquist–Majda condition is of much less accuracy. It



**Fig. 2:** Typical snapshots of the reference solution  $u^*$  and the solutions  $u|_{ABC_{EM}^{1,1}}$ ,  $u|_{ABC_{PS}^{1,0}}$ ,  $u|_{ABC_{PS}^{1,1}}$  affected by reflected waves from the first order Engquist–Majda condition, zero and first order ABCs based on the pseudo-differential calculus, respectively. The excitation frequency is  $\omega = 100$  kHz.

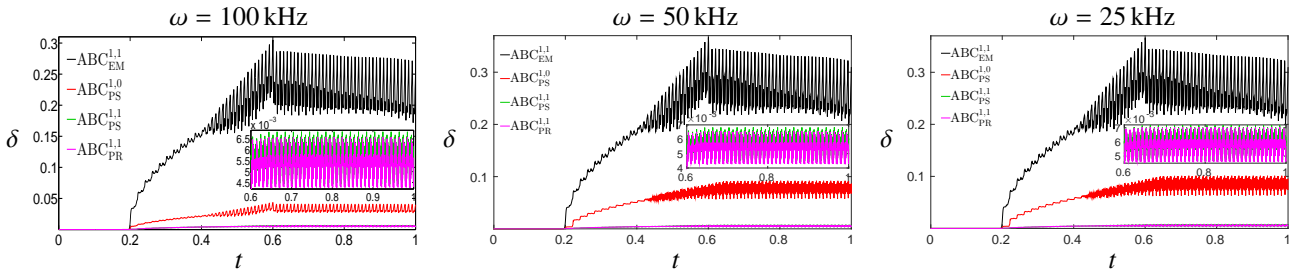


**Fig. 3:** One dimensional waveguide. Relative error  $\delta$  versus time  $t$  for different excitation frequencies  $\omega$  and for the first ( $ABC_{EM}^{1,1}$ ) order Engquist–Majda condition, zero ( $ABC_{PS}^{1,0}$ ) and first ( $ABC_{PS}^{1,1}$ ) order boundary conditions based on the pseudo-differential calculus, and the first order para-differential condition ( $ABC_{PR}^{1,1}$ ). Note that the rectangular in the right down corner is a magnification of the lower part of the graph.

416 also has an initial growing trend for  $t \in [0.2, 0.6]$ , which is, however, much steeper than that of the conditions  $ABC_{PS}^{1,0}$ ,  
 417  $ABC_{PS}^{1,1}$ , and the fluctuations are significantly larger.

418 We would like to draw the reader’s attention to the resemblance between the error plots for  $ABC_{PS}^{1,0}$  and  $ABC_{EM}^{1,1}$ :  
 419 the local disturbance at  $t = 0.6$  on both graphs (noticeable for  $ABC_{EM}^{1,1}$ , and barely perceptible for  $ABC_{PS}^{1,0}$ ), as well  
 420 as the declined trend for  $t > 0.6$ . By analyzing the reflected waves for the boundary conditions  $ABC_n^{1,0}$  ( $\sigma = \{0, 1\}$ ,  
 421  $n = \{EM, PS, PR\}$ ) we found that  $\bar{\delta}(u^*, u|_{ABC_{EM}^{1,1}}) \approx \bar{\delta}(u^*, u|_{ABC_{PS}^{1,0}})$  in the sense that their extrema evolve in a similar way  
 422 and appear essentially at the same instances in time (Fig. 4). Although  $ABC_{EM}^{1,1}$  and  $ABC_{PS}^{1,0}$  are quantitatively different,  
 423 their qualitative resemblance is evident. In effect, such a similarity is not a coincidence. These boundary conditions are  
 424 very similar in form, and  $ABC_{EM}^{1,1}$  can be derived analogously to  $ABC_{PS}^{1,0}$  by taking  $u^{(0)} = 0$  in the linearized Westervelt

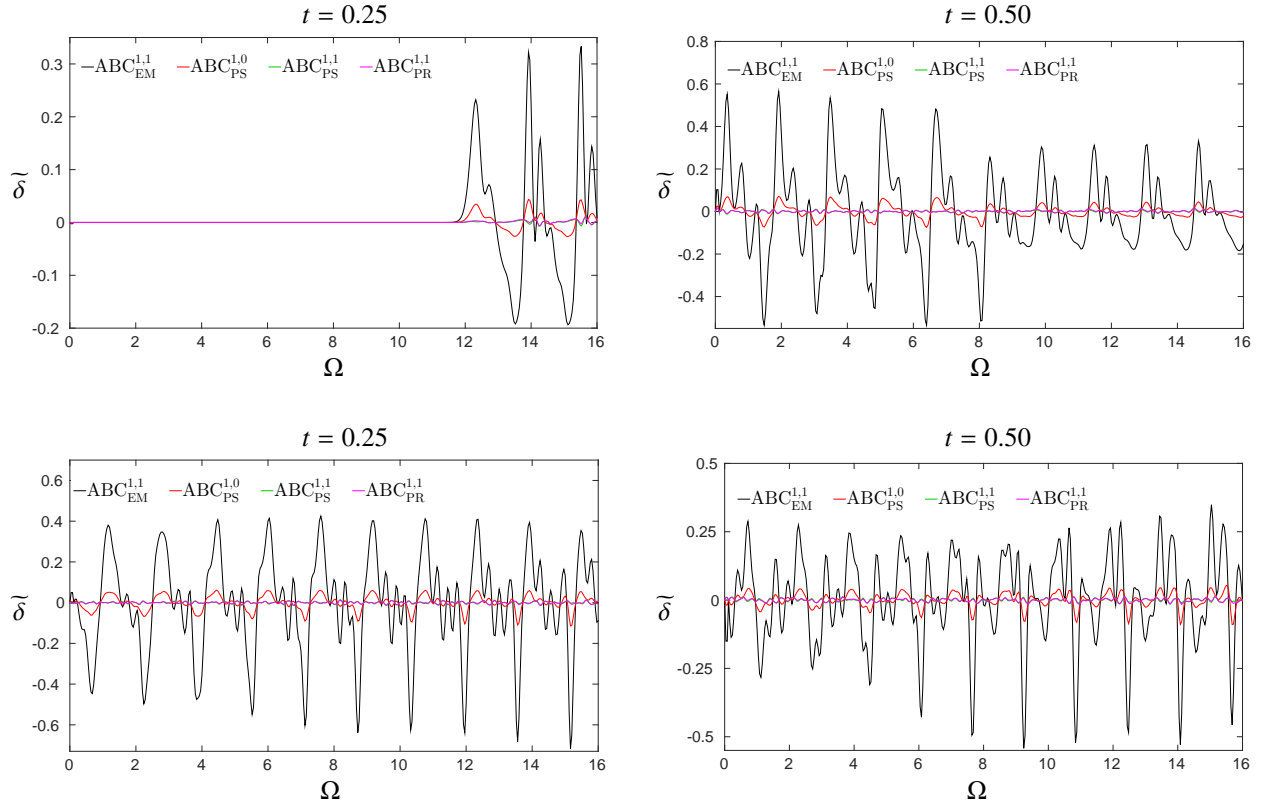


**Fig. 4:** One dimensional waveguide. Typical snapshots of the difference  $\tilde{\delta} = u^* - u$  (vertical axis) between the reference solution  $u^*$  and the solution  $u$  distorted by reflected waves from the first (ABC<sub>EM</sub><sup>1,1</sup>) order Engquist–Majda condition, zero (ABC<sub>PS</sub><sup>1,0</sup>) and first (ABC<sub>PS</sub><sup>1,1</sup>) order boundary conditions based on the pseudo-differential calculus, and the first order para-differential condition (ABC<sub>PR</sub><sup>1,1</sup>).

425 equation (46). However, the boundary conditions ABC<sub>PS</sub><sup>1,1</sup> and ABC<sub>PR</sub><sup>1,1</sup> work differently and possess similarity with  
 426 neither of the two mentioned.

## 427 5.2. ABC in 2-d

428 In this part we study how the boundary conditions with ABC<sub>n</sub><sup>2,o</sup>,  $o = \{0, 1\}$ ,  $n = \{\text{PS}, \text{PR}, \text{EM}\}$  absorb ultrasound  
 429 waves at different frequencies and angles of incidence in a two-dimensional horizontal acoustic waveguide and also  
 430 analyze the performance of the ABCs for the High-Intensity Focused Ultrasound problem.

### 431 5.2.1. Acoustic waveguide

432 We consider a two-dimensional horizontal acoustic waveguide  $\Omega \in [0, 8 \text{ cm}] \times [0, 18 \text{ cm}]$  and the excitation  $u_n$   
 433 with a frequency  $\omega = \{25, 50, 100\}$  kHz set on the left boundary  $\Gamma_N$  of the domain  $\Omega$ . The ABC studied was prescribed  
 434 on the right boundary  $\Gamma_A$ , which is inclined to the horizontal axis at one of the angles  $\alpha = \{75^\circ, 60^\circ, 45^\circ\}$  (Fig. 5).

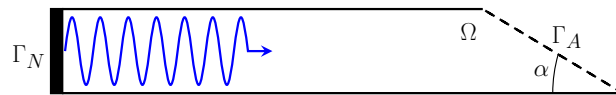


**Fig. 5:** General geometric setup for the horizontal acoustic waveguide  $\Omega$ .

435 A series of snapshots of the reference solution  $u^*$  and the solution affected by the boundary conditions ABC<sub>n</sub><sup>2,o</sup>  
 436 ( $o = \{0, 1\}$ ,  $n = \{\text{PS}, \text{EM}\}$ ) are shown in Fig. 6. In this case, the situation is essentially the same as for the 1-  
 437 d waveguide. The Engquist–Majda condition of first order significantly pollutes the solution with reflected waves

438 (Fig. 6(b)). The second order Engquist–Majda ABC outperforms the first order one, but the reflections are still very  
439 large (Fig. 6(c)). Per contra, the zero order condition  $ABC_{PS}^{2,0}$  exhibits a much better performance and only introduces  
440 low-amplitude reflected waves into the solution (Fig. 6(d)). The first order conditions  $ABC_{PS}^{2,1}$  and  $ABC_{PR}^{2,1}$  demonstrate  
441 a considerable improvement and a very accurate solution compared to the conditions  $ABC_{EM}^{2,1}$ ,  $ABC_{EM}^{2,2}$  and  $ABC_{PS}^{2,0}$   
442 (Fig. 6(e)). We did not present the results for the boundary condition  $ABC_{PR}^{2,1}$  derived via the para-differential approach,  
443 since, as in the one-dimensional case, it gives essentially the same accuracy as  $ABC_{PS}^{2,1}$ .

444 The dependency of the ABCs, considered in this section, on the excitation frequency  $\omega$  echoes that of the ABCs  
445 in 1-d case - there is no considerable loss of accuracy when  $\omega$  changes (Fig. 7). On the contrary, the incident angle  $\alpha$   
446 significantly affects the performance of the ABCs. As  $\alpha$  decreases, so does the accuracy, and this effect is more pro-  
447 nounced for the first and second order Engquist–Majda boundary conditions. The proposed ABCs are less influenced  
448 by the angle of incidence compared to the Engquist–Majda conditions and still give relatively accurate results even in  
449 low- $\alpha$  regimes.

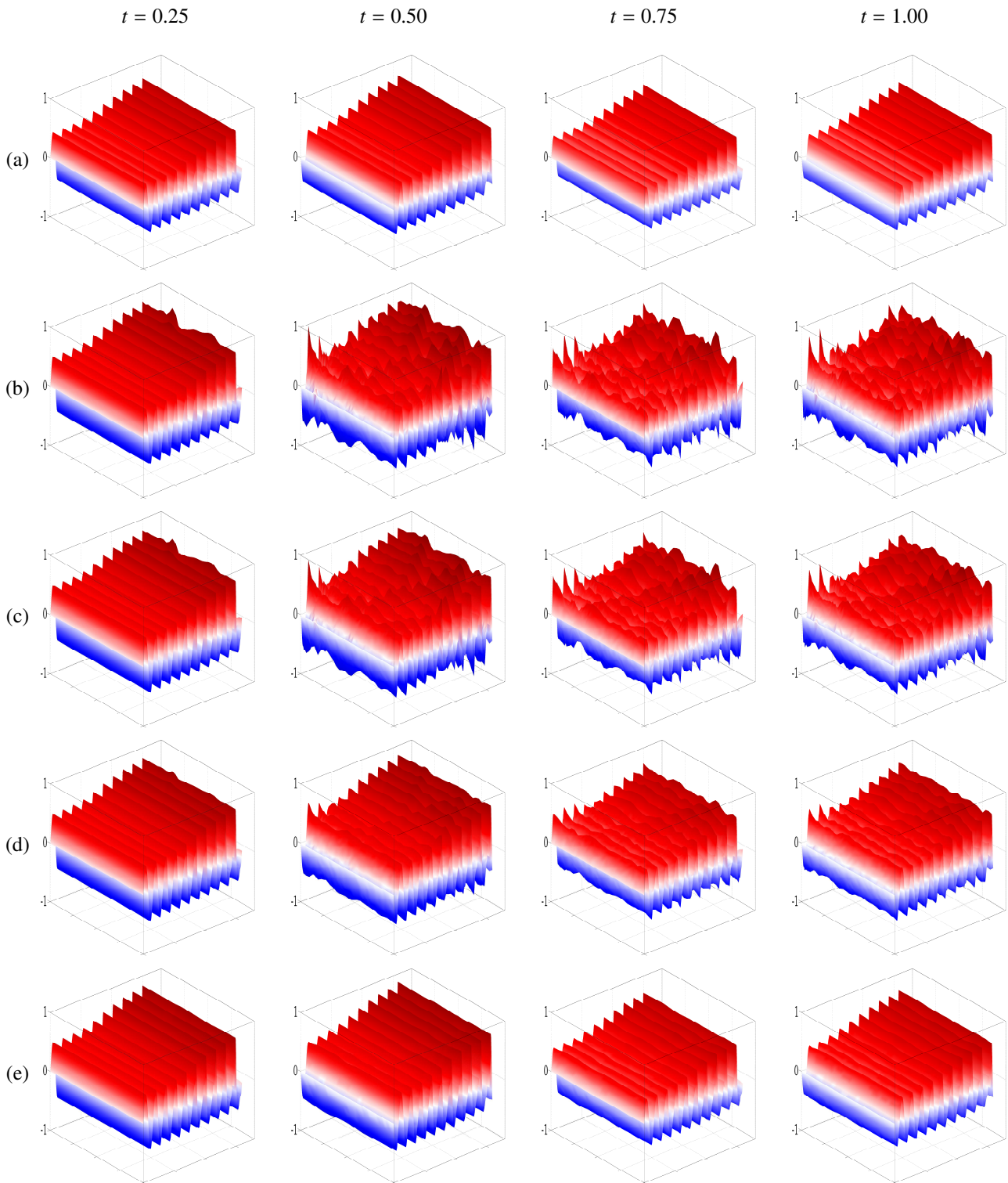


**Fig. 6:** Typical snapshots of the solution in the 2-d waveguide with  $\alpha = 75^\circ$  and  $\omega = 100$  kHz: (a) the reference solution  $u^*$ ; and the solution  $u$  distorted by reflect waves from the boundary conditions (b)  $ABC_{EM}^{2,1}$ , (c)  $ABC_{EM}^{2,2}$ , (d)  $ABC_{PS}^{2,0}$ , (e)  $ABC_{PS}^{2,1}$ .

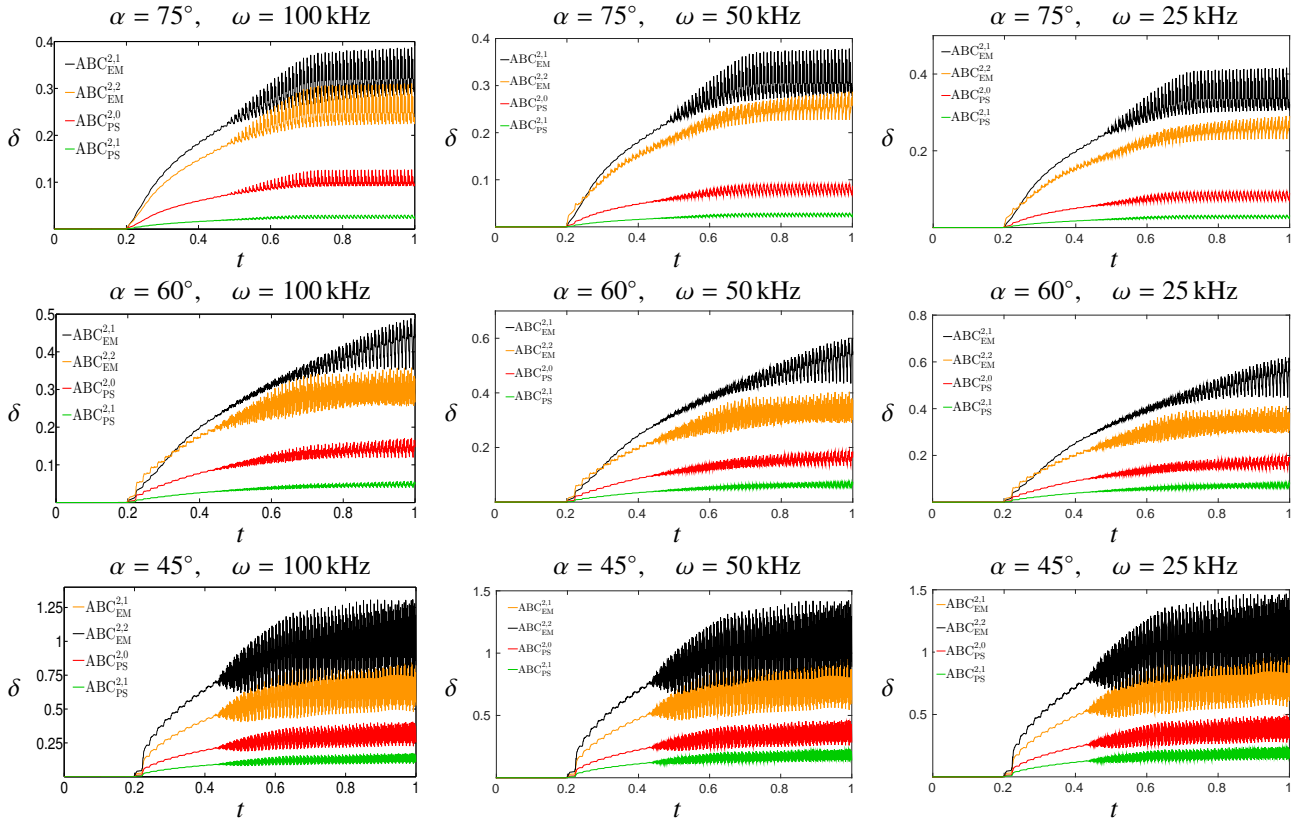


**Fig. 7:** Dependency of the relative error  $\delta$  on the excitation frequency  $\omega$  and the incidence angle  $\alpha$  in the two dimensional waveguide. Relative error  $\delta$  versus time  $t$  for the first ( $ABC_{EM}^{2,1}$ ) and second ( $ABC_{EM}^{2,2}$ ) order Engquist–Majda conditions, and for the zero ( $ABC_{PS}^{2,0}$ ) and first ( $ABC_{PS}^{2,1}$ ) order boundary conditions based on the pseudo-differential calculus.

### 5.2.2. High-Intensity Focused Ultrasound problem

In this part, we studied the HIFU problem in which we used monofrequency excitation by a concave array of transducers, with an aperture of 20 mm and excitation frequency  $\omega = 1.0$  MHz, located on the bottom of the domain  $\Omega$  (Fig. 8). Such a transducer array shape allows to focus high intensity ultrasound waves on the desired place within the sonicated biotissue and create a local temperature increase to destroy tumor cells. On the rest of the boundary  $\Gamma_A$  we set the ABC studied. The configuration of the computational domain used as well as the transducer characteristics and the problem parameters are typical for numerical simulations of HIFU ablations of tumors.

The accuracy of ABCs for the HIFU problem is one of the most important issues, since in case of using inaccurate ABCs reflected waves can significantly contaminate the acoustic pressure field, which, in turn, is used in the coupled thermo-acoustic HIFU problem to compute the temperature distribution in the sonicated biotissue. The knowledge of the temperature field determines the success of any HIFU therapy and therefore its distortion can lead to misinterpretation of simulation results.

The reference solution  $u^*$  and the solution  $u$  influenced by reflected waves from the boundary conditions  $ABC_n^{2,0}$  ( $o = \{0, 1\}$ ,  $n = \{EM, PS\}$ ) at different characteristic time steps are shown in Fig. 9.

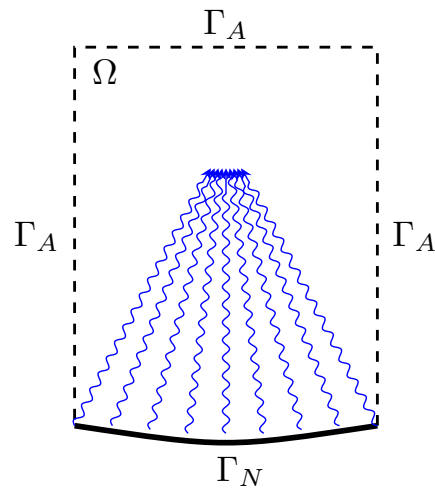


**Fig. 8:** General geometric setup for the high-intensity focused ultrasound problem.



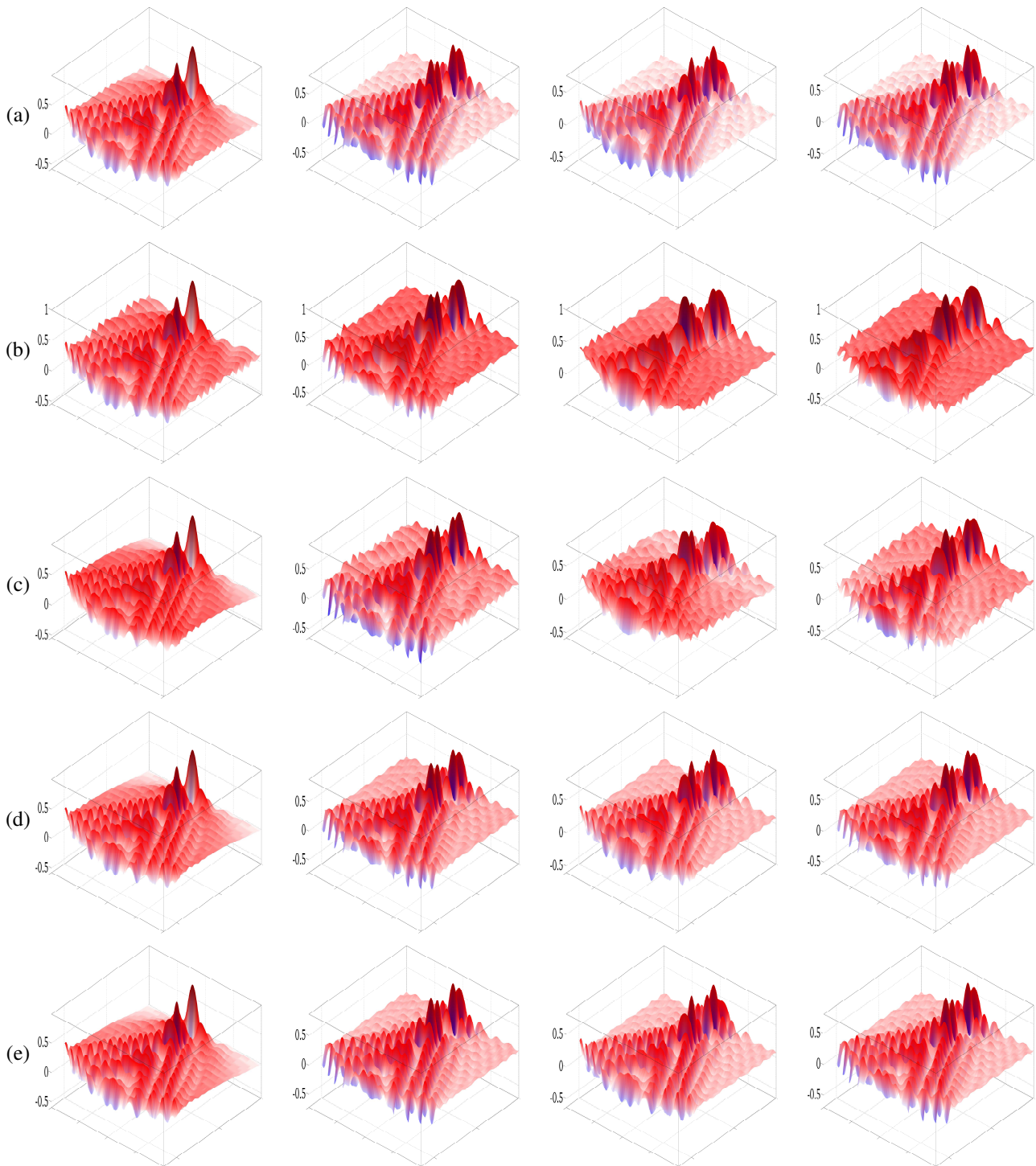


**Fig. 9:** Snapshots of the solution for the HIFU problem: (a) the reference solution  $u^*$ ; and the solution  $u$  distorted by reflect waves from the boundary conditions (b)  $ABC_{EM}^{2,1}$ , (c)  $ABC_{EM}^{2,2}$ , (d)  $ABC_{PS}^{2,0}$ , (e)  $ABC_{PS}^{2,1}$ .

464 The difference between these boundary conditions is clearly visible. In particular, the second order Engquist–  
 465 Majda ABC outperforms the first order one, especially in the focal spot, where the solution is affected the most by the



466 reflected waves (Figs.9(b) and 9(c)). Interestingly that far off the focus the first order Engquist–Majda ABC seems to  
 467 perform even better than its second order version. However, overall the second order Engquist–Majda condition gives  
 a better accuracy as opposed to the first order one.

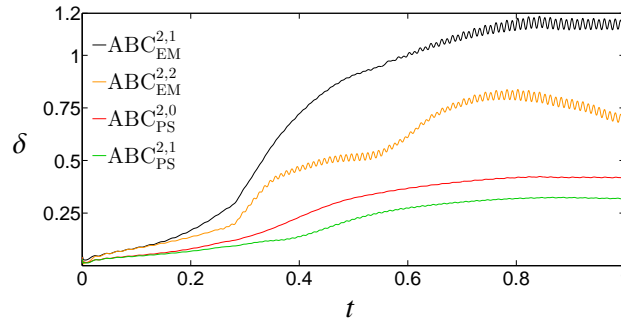


**Fig. 10:** HIFU problem. Relative error  $\delta$  versus time  $t$  for the first ( $ABC_{EM}^{2,1}$ ) and second ( $ABC_{EM}^{2,2}$ ) order Engquist–Majda conditions, and for the zero ( $ABC_{PS}^{2,0}$ ) and first ( $ABC_{PS}^{2,1}$ ) order boundary conditions based on the pseudo-differential calculus.

468 The proposed ABCs of zero and first order demonstrate much more accurate results than the Engquist–Majda  
 469 ABCs in both the focal zone and in the periphery of the computational domain (Figs.9(d) and 9(e)). Moreover, they  
 470 also show a much smoother behaviour in time, which is confirmed by the relative error  $\delta$  (Fig. 10).  
 471

## 472 6. Conclusions

473 In this work we have proposed local in space and time absorbing boundary conditions for the Westervelt equation  
 474 in one and two space dimensions. The derivation of the boundary conditions is based on the theory of pseudo-  
 475 and para-differential calculus, which has been applied to the construction of absorbing boundary conditions for the  
 476 Westervelt equation in this work for the first time. We have found that both techniques lead to essentially the same  
 477 absorbing boundary conditions in terms of computational efficiency and numerical accuracy.

478 We have studied different approaches to the linearization of the Westervelt equation (the Taylor linearization,  
 479 asymptotic expansions, and the Bony para-linearization) and found that they are all equivalent if the Taylor lineariza-  
 480 tion uses the same assumption as the para-linearization approach - the function vanishes at the reference solution.

481 All our numerical tests exhibit no instabilities, and demonstrate both the efficiency and effectiveness of the pro-  
 482 posed boundary conditions. They are also attractive from the computational point of view due to their local character  
 483 and are easy to implement into existing numerical methods. The developed absorbing boundary conditions provide  
 484 quantitatively much better results than the classical first and second order Engquist–Majda conditions and can effi-  
 485 ciently handle different regimes of wave propagation in a wide range of excitation frequencies and angles of incidence.  
 486 This shows that it pays off to take into account the nonlinearity as well as strong damping present in the Westervelt  
 487 equation also in the boundary conditions. It is also important to remark that the application of the self-adapting  
 488 technique [49] to the proposed boundary conditions will result in further improvements.

## 489 7. Acknowledgments

490 The first author would like to thank EPSRC Mathematics Platform grant EP/I019111/1 for the partial support  
 491 of this work. The second author gratefully acknowledges support by the Austrian Science Fund (FWF) under the  
 492 grant P24970. We thank Barbara Wohlmuth, TU Munich, and Manfred Kaltenbacher, TU Vienna, for stimulating  
 493 discussions.

## 494 References

- 495 [1] S. Abarbanel, D. Gottlieb, and J. S. Hesthaven. Wellposed perfectly matched layers for advective acoustics. *J. Comput. Phys.*, 154(2):266–  
 496 283, 1999.

- 497 [2] S. Abarbanel, D. Gottlieb, and J. S. Hesthaven. Long time behavior of the perfectly matched layer equations in computational electromag-  
498 netics. *J. Sci. Comput.*, 17(1-4):405–422, 2002.
- 499 [3] X. Antoine and H. Barucq. Microlocal diagonalization of strictly hyperbolic pseudodifferential systems and application to the design of  
500 radiation conditions in electromagnetism. *SIAM J. Appl. Math.*, 61(6):1877–1905, 2001.
- 501 [4] D. Appelö, T. Hagstrom, and G. Kreiss. Perfectly matched layers for hyperbolic systems: general formulation, well-posedness, and stability.  
502 *SIAM J. Appl. Math.*, 67(1):1–23, 2006.
- 503 [5] D. Appelö and G. Kreiss. Application of a perfectly matched layer to the nonlinear wave equation. *Wave Motion*, 44(7-8):531–548, 2007.
- 504 [6] M. Averkiou and R. Cleveland. Modeling of an electrohydraulic lithotripter with the KZK equation. *J. Acoust. Soc. Am.*, 106(1):102–112,  
505 1999.
- 506 [7] H. Barucq, C. Bekkey, and R. Djellouli. Construction of local boundary conditions for an eigenvalue problem using micro-local analysis:  
507 application to optical waveguide problems. *J. Comput. Phys.*, 193(2):666–696, 2004.
- 508 [8] H. Barucq, J. Diaz, and V. Duprat. Micro-differential boundary conditions modelling the absorption of acoustic waves by 2d arbitrarily-shaped  
509 convex surfaces. *Commun. Comput. Phys.*, 11(2):674–690, 2012.
- 510 [9] H. Barucq, J. Diaz, and M. Tlemcani. New absorbing layers conditions for short water waves. *J. Comput. Phys.*, 229(1):58–72, 2010.
- 511 [10] E. Bécache, D. Givoli, and T. Hagstrom. High-order absorbing boundary conditions for anisotropic and convective wave equations. *J.*  
512 *Comput. Phys.*, 229(4):1099–1129, 2010.
- 513 [11] J.-P. Berenger. A perfectly matched layer for the absorption of electromagnetic waves. *J. Comput. Phys.*, 114(2):185–200, 1994.
- 514 [12] J. Chung and G.M. Hulbert. A time integration algorithm for structural dynamics with improved numerical dissipation: The generalized  
515  $\alpha$ -method. *J. Appl. Mech.*, 60(2):371–375, 1993.
- 516 [13] C. Clason, B. Kaltenbacher, and S. Veljovic. Boundary optimal control of the Westervelt and the Kuznetsov equations. *J. Math. Anal. Appl.*,  
517 356(2):738–751, 2009.
- 518 [14] G. C. Cohen. *Higher-Order Numerical Methods for Transient Wave Equations*. Springer, 2002.
- 519 [15] C.W. Connor and K. Hynynen. Bio-acoustic thermal lensing and nonlinear propagation in focused ultrasound surgery using large focal spots:  
520 a parametric study. *Phys. Med. Biol.*, 47(11):1911–1928, 2002.
- 521 [16] J. Diaz and P. Joly. A time domain analysis of PML models in acoustics. *Comput. Methods Appl. Mech. Engrg.*, 195(29–32):3820–3853,  
522 2006.
- 523 [17] T. Dreyer, W. Kraus, E. Bauer, and R. E. Riedlinger. Investigations of compact self focusing transducers using stacked piezoelectric elements  
524 for strong sound pulses in therapy. In *Proceedings of the IEEE Ultrasonics Symposium*, pages 1239–1242, 2000.
- 525 [18] E. Dubach. Nonlinear artificial boundary conditions for the viscous Burgers equation. Technical Report 00/04, preprint of université de Pau  
526 et des pays de l'Adour, 2000.
- 527 [19] B. Engquist and A. Majda. Absorbing boundary conditions for the numerical simulation of waves. *Math. Comp.*, 31(139):629–651, 1977.
- 528 [20] B. Engquist and A. Majda. Radiation boundary conditions for acoustic and elastic wave calculations. *Comm. Pure Appl. Math.*, 32(3):313–  
529 357, 1979.
- 530 [21] C. Le Floch and M. Fink. Ultrasonic mapping of temperature in hyperthermia: the thermal lens effect. In *Proceedings of 1997 IEEE*  
531 *Ultrasonics Symposium*, pages 1301–1304, 1997.
- 532 [22] C. Le Floch, M. Tanter, and M. Fink. Self-defocusing in ultrasonic hyperthermia: Experiment and simulation. *Appl. Phys. Lett.*, 74(20):3062–  
533 3064, 1999.
- 534 [23] D. Givoli. Non-reflecting boundary conditions. *J. Comput. Phys.*, 94(1):1–29, 1991.
- 535 [24] D. Givoli. High-order local non-reflecting boundary conditions: a review. *Wave motion*, 39(4):319–326, 2004.
- 536 [25] D. Givoli. Computational absorbing boundaries. In S. Marburg and B. Nolte, editors, *Computational Acoustics of Noise Propagation in*  
537 *Fluids*, chapter 5, pages 145–166. Springer-Verlag, Berlin Heidelberg, 2008.
- 538 [26] T. Hagstrom. Radiation boundary conditions for the numerical simulation of waves. *Acta Numerica*, 8:47–106, 1999.
- 539 [27] T. Hagstrom. New results on absorbing layers and radiation boundary conditions. In M. Ainsworth, P. Davies, D. Duncan, P. Martin, and  
540 B. Rynne, editors, *Topics in computational wave propagation. Direct and inverse problems. Lect. Notes Comput. Sci. Eng.*, volume 31, pages  
541 1–42. Springer-Verlag, New York, 2003.
- 542 [28] I.M. Hallaj, R.O. Cleveland, and K. Hynynen. Simulations of the thermo-acoustic lens effect during focused ultrasound surgery. *J. Acoust.*  
543 *Soc. Am.*, 109(5):2245–2253, 2001.
- 544 [29] M.F. Hamilton and D.T. Blackstock. *Nonlinear acoustics*. Academic Press, 1998.
- 545 [30] G. W. Hedstrom. Nonreflecting boundary conditions for nonlinear hyperbolic systems. *J. Comput. Phys.*, 30(2):222–237, 1979.
- 546 [31] J. S. Hesthaven. On the analysis and construction of perfectly matched layers for the linearized Euler equations. *J. Comput. Phys.*, 142(1):129–  
547 147, 1998.
- 548 [32] L. Hörmander. Pseudo-differential operators. *Commun. Pure Appl. Math.*, 18(3):501–517, 1965.
- 549 [33] L. Hörmander. *The analysis of linear partial differential operators III: Pseudo-Differential Operators*. Springer-Verlag, Berlin Heidelberg,  
550 1985.
- 551 [34] Fang Q. Hu. A stable, perfectly matched layer for linearized Euler equations in unsplit physical variables. *J. Comput. Phys.*, 173(2):455–480,  
552 2001.
- 553 [35] T. Hughes. *The finite element method: linear static and dynamic finite element analysis*. Prentice-Hall, 1987.
- 554 [36] J.M. Bony. Calcul symbolique et propagation des singularités pour les équations aux dérivées partielles non linéaires. *Ann.Sc.E.N.S. Paris*,  
555 14:209–246, 1981.
- 556 [37] B. Kaltenbacher and I. Lasiecka. Global existence and exponential decay rates for the Westervelt equation. *Discrete and Continuous*  
557 *Dynamical Systems (DCDS)*, 2:503–525, 2009.
- 558 [38] B. Kaltenbacher and I. Shevchenko. Well-posedness of the Westervelt equation with higher order absorbing boundary conditions. 2015. In  
559 preparation.
- 560 [39] M. Kaltenbacher. *Numerical simulation of mechatronic sensors and actuators*. 2nd Edition, Springer, Berlin, 2007.
- 561 [40] J. Kohn and L. Nirenberg. An algebra of pseudo-differential operators. *Commun. Pure Appl. Math.*, 18(1-2):269–305, 1965.

- 562 [41] T. Lähivaara and T. Huttunen. A non-uniform basis order for the discontinuous Galerkin method of the 3D dissipative wave equation with  
563 perfectly matched layer. *J. Comput. Phys.*, 229(13):5144–5160, 2010.
- 564 [42] M.J. Lighthill. Viscosity effects in sound waves of finite amplitude. In *Surveys in mechanics*, pages 250–351. Cambridge University Press,  
565 1956.
- 566 [43] A. Majda and S. Osher. Reflection of singularities at the boundary. *Comm. Pure Appl. Math.*, 28(4):479–499, 1975.
- 567 [44] Y. Meyer. Remarques sur un théorème de j.m. bony. *Suppl. ai Rend. del Circolo mat. di Palermo*, 2:1–20, 1981.
- 568 [45] L. Nirenberg. Lectures on linear partial differential equations. *Uspekhi Mat. Nauk*, 30(4):147–204, 1975.
- 569 [46] R. R. Paz, M. A. Storti, and L. Garelli. Absorbing boundary condition for nonlinear hyperbolic partial differential equations with unknown  
570 Riemann invariants. *Fluid Mechanics (C)*, XXVIII(19):1593–1620, 2009.
- 571 [47] M. Pernot, K.R. Waters, J. Bercoff, M. Tanter, and M. Fink. Reduction of the thermo-acoustic lens effect during ultrasound-based temperature  
572 estimation. In *Proceedings of 2002 IEEE Ultrasonics Symposium*, pages 1447–1450, 2002.
- 573 [48] O.V. Rudenko and S.I. Soluyan. *Theoretical foundations of nonlinear acoustics*. Consultants Bureau, a division of Plenum Publishing  
574 Corporation, 1977.
- 575 [49] I. Shevchenko and B. Wohlmuth. Self-adapting absorbing boundary conditions for the wave equation. *Wave Motion*, 49(4):461–473, 2012.
- 576 [50] C. Simon, P. VanBaren, and E.S. Ebbini. Two-dimensional temperature estimation using diagnostic ultrasound. *IEEE Trans. Ultrason. Ferr.*,  
577 45(4):1088–1099, 1998.
- 578 [51] J. Szeftel. Absorbing boundary conditions for nonlinear scalar partial differential equations. *Comput. Method. Appl. M.*, 195(29-32):3760–  
579 3775, 2006.
- 580 [52] J. Szeftel. A nonlinear approach to absorbing boundary conditions for the semilinear wave equation. *Math. Comput.*, 75(254):565–594, 2006.
- 581 [53] S. Tsynkov. Numerical solution of problems on unbounded domains. A review. *Appl. Numer. Math.*, 27(4):465–532, 1998.
- 582 [54] T. Varslot and G. Taraldsen. Computer simulation of forward wave propagation in soft tissue. *IEEE Trans. Ultrason. Ferroelectr. Freq.*  
583 *Control*, 52(9):1473–1482, 2005.
- 584 [55] P. J. Westervelt. Parametric acoustic array. *J. Acoust. Soc. Am.*, 35(4):535–537, 1963.
- 585 [56] B. Wohlmuth. A mortar finite element method using dual spaces for the Lagrange multiplier. *SIAM J. Numer. Anal.*, 38(3):989–1012, 2001.
- 586 [57] B. Wohlmuth. A comparison of dual Lagrange multiplier spaces for mortar finite element discretizations. *M2AN Math. Model. Numer. Anal.*,  
587 36(6):995–1012, 2002.
- 588 [58] M. W. Wong. *An introduction to pseudo-differential operators*. World Scientific Publishing, Singapore, 1999.
- 589 [59] J. Zhang, Z. Xu, and X. Wu. Unified approach to split absorbing boundary conditions for nonlinear Schrödinger equations: Two-dimensional  
590 case. *Phys. Rev. E*, 79(4):046711–1–046711–8, 2009.